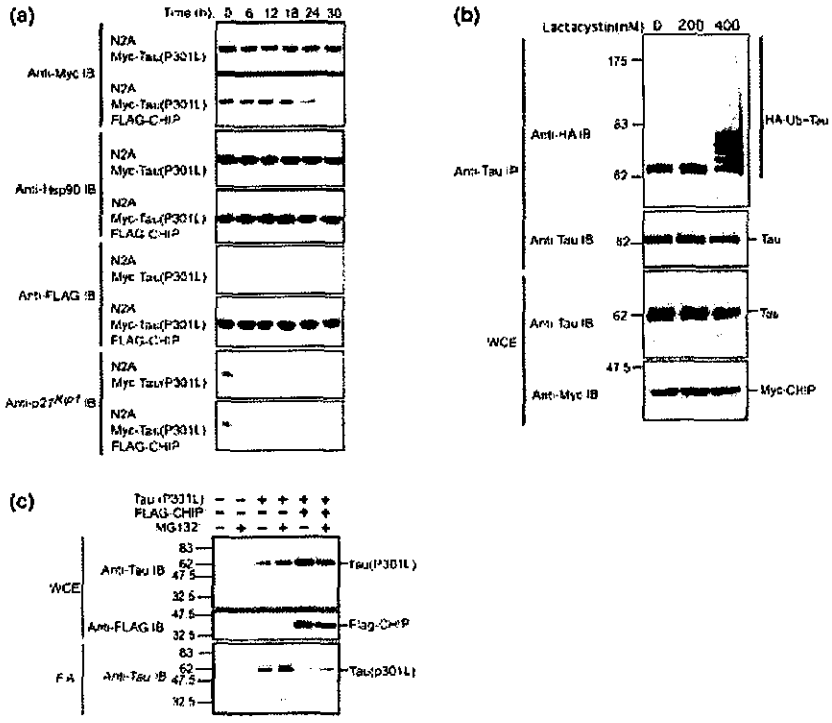

Fig. 3 Carboxyl terminus of Hsc70-interacting protein (CHIP) implicated in the regulation of neuronal cell death. (a) Cycloheximide-chase analysis of tau (P301L) with CHIP. The stably expressed Neuro2A cell lines with Myc-tau (P301L) and FLAG-CHIP were established by infection of retrovirus with cDNA encoding Myc-tau (P301L) and FLAG-CHIP and by puromycin selection. Cells were cultured with cycloheximide at a concentration of 50 μg/mL and then incubated for various times (0, 6, 12, 18, 24 and 30 h). Cell lysates were then subjected to sodium dodecyl sulfate–polyacrylamide gel electrophoresis (SDS–PAGE) and immunoblot analysis was performed with antibody to Myc, Hsp90, FLAG and $p27^{Kip1}$. The anti-$p27^{Kip1}$ immunoblot shows that cycloheximide is active. (b) Effects of treatment with the proteasome inhibitor lactacystin. HEK293 cells expressing tau, CHIP and HA-tagged ubiquitin (HA-Ub) were treated with various concentrations of lactacystin for 14 h, the cell lysates were immunoprecipitated with anti-tau monoclonal antibody and an anti-HA immunoblot was performed to detect the ubiquitylation on tau. (c) Soluble or insoluble fraction of Tau (P301L). The soluble (WCE) or insoluble [formic acid (FA)] fraction from cells expressing Tau (P301L) with or without FLAG-CHIP was separated with or without treatment with MG135. The fractions were subjected to SDS–PAGE and immunoblot analysis was performed with antibody to tau and FLAG. Hsp90 as internal control.

MG132, a potent inhibitor of proteasome (Fig. 3c, lanes 3 and 4). Coexpression with CHIP sustained the amount of the SDS-soluble tau fraction and significantly inhibited the formation of SDS-insoluble tau. MG132 treatment enhanced the formation of SDS-insoluble tau but the amount recovered was still much lower than that from cells where CHIP was not coexpressed (Fig. 3c, lanes 5 and 6). These results indicate that the inhibition of SDS-insoluble tau formation stems from the role of CHIP in the degradation of tau. Thus, CHIP may be involved in NFT formation.

Many suspect a possible connection between NFT formation and neuronal death in neurodegenerative diseases because neuronal loss is also common in areas where NFTs are observed. Therefore, we investigated the possible role of CHIP in connecting NFT formation and cell death. We first established cell lines that knocked down endogenous CHIP using a vector-based RNA interference (RNAi) technique (Fig. 4a). CHIP RNAi expression blocked the expression of endogenous CHIP but did not affect the expression of Hsp90. Green fluorescent protein (GFP) RNAi also did not affect CHIP expression. Tau (P301) over-expression had no affect on the cell viability of Neuro2A, even though SDS-insoluble tau was formed. Stable cell lines were incubated with the proteasome inhibitor MG132 (20 μM) for 24 h and then alive or dead cells were determined by trypan blue exclusion (Fig. 4b). This treatment induced cell death in 50% of the non-treated cells in GFP RNAi-expressing cells, CHIP-overexpressing cells and mock cells. The RNAi inhibition of CHIP and the expression of tau (P301L) facilitated an MG132-induced cell death of 70% of untreated cells and CHIP overexpression restored the cell death level to that of cells with no tau expression (Fig. 4b). Therefore, CHIP is involved in tau (P301L)-mediated, MG132-induced cell death. It should be noted that, although CHIP expression prevented neurons from undergoing proteasome inhibition-induced neuronal death, surviving neurons still showed SDS-insoluble tau (Fig. 3c) which suggests the development of

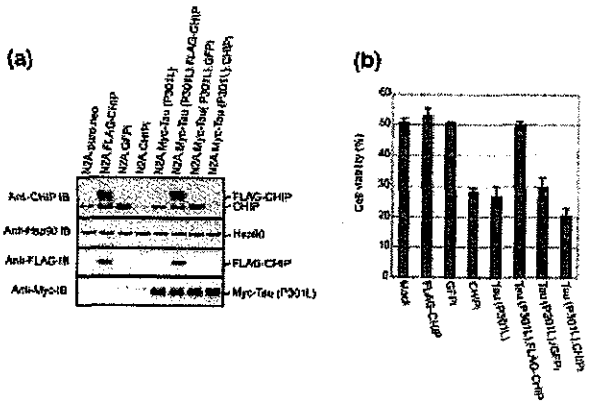

Fig. 4 Carboxyl terminus of Hsc70-interacting protein (CHIP) as a critical factor to protect from stress by proteasome inhibitor. (a) Reduced amounts of CHIP in cells with CHIP RNA interference (RNAi) but not EGFP RNAi. Neuro2A cells were treated with retrovirus vector-based RNAi for CHIP or EGFP and then selected with puromycin. These cell lines were further infected by retrovirus with Myc-tau (P031L) and neo^R and then selected with puromycin and G418. Double-infected cell lines were used for immunoblot with antibodies to CHIP, FLAG, Myc and Hsp90 as internal control. (b) Stable Neuro2A cell lines were cultured with 20 μM MG132, incubated for 24 h and the cell number was counted after trypan blue staining. The amounts of CHIP in cells with CHIP but not EGFP RNAi were reduced. Neuro2A cells were treated with retrovirus vector-based RNAi for CHIP or EGFP and then selected with puromycin.

NFT formation. This was verified by neuropathological staining in which CHIP colocalized in NFTs of progressive supranuclear palsy brain (Fig. 5), mostly containing four-repeat tau, and also reacted to anti-ubiquitin antibody. The most NFT-bearing cells were stained by the anti-CHIP antibody in progressive supranuclear palsy brain but very faintly stained in Alzheimer's disease (AD) brain (data not shown).

Discussion

In this study, we have shown that the U-box protein CHIP is a tau-interacting protein *in vivo* and that CHIP mediates poly-ubiquitylation preferentially on four-repeat tau as a ubiquitin ligase followed by degradation by proteasome. In the *in vitro* ubiquitination assay, molecular chaperones such as Hsp90 or Hsc70 or hyperphosphorylation of tau are not required for CHIP-mediated tau ubiquitylation (Fig. 1d). To date, CHIP has been shown to bind to a subset of chaperone substrates, including glucocorticoid receptor, cystic fibrosis transmembrane conductance regulator and ErbB2, suggesting that CHIP has sensor functions that recognize different kinds of misfolded proteins (Connell *et al.* 2001; Meacham *et al.* 2001; Imai *et al.* 2002; Xu *et al.* 2002). In *in vivo* conditions, Hsp might support the CHIP-mediated tau ubiquitylation and degradation because tau was not accumulated in neurons exhibiting an increased level of Hsp90 (Dou *et al.* 2003). To

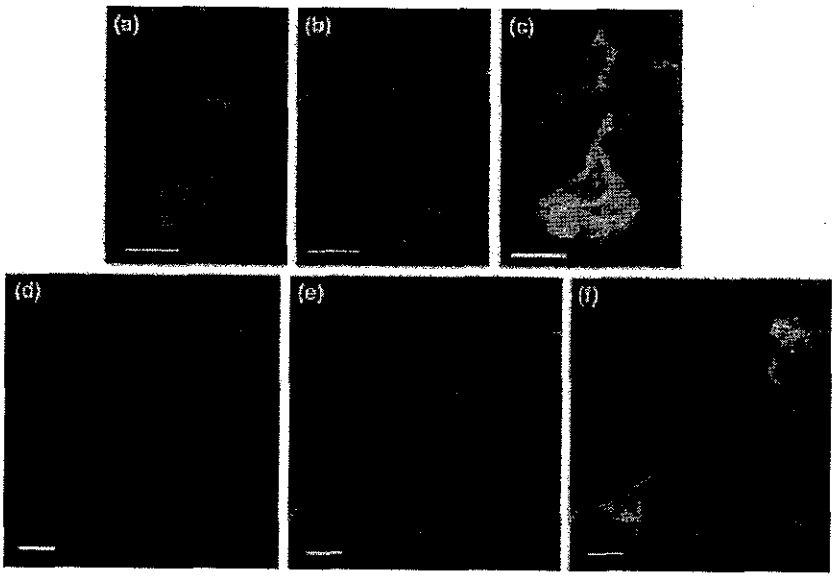

Fig. 5 Neuropathological analysis in progressive supranuclear palsy (PSP). Neurons in PSP brain were stained with anti-carboxyl terminus of Hsc70-interacting protein (CHIP; green; a and d) and anti-phosphorylated tau (AT8; orange; b and e). (c and f) Merged image of both anti-CHIP and AT8 immunoreactivities. Brains were immersion fixed with 10% buffered formalin and paraffin-embedded sections (2–10 μm) were prepared for confocal microscopic analyses. Deparaffinized sections were treated in either 0.1% Triton X-100 in phosphate-buffered saline for 20 min or Target Retrieval Solution (Dako). AT8 and anti-CHIP were used as primary antibodies and then incubated with either Alexa488/568-conjugated anti-mouse IgG or Alexa488/568-conjugated anti-rabbit IgG. Sections were then examined with a Radiance 2000 KR3 confocal microscope (Bio-Rad). Scale bars, 10 μm.

uncover how CHIP recognizes and ubiquitylates tau without molecular chaperones, it is first necessary to understand the structural basis for this significant function.

Phosphorylated tau was reported to preferentially ubiquitylate in COS cells (Shimura *et al.* 2003). In our experiments, four-repeat tau was ubiquitylated by CHIP without phosphorylation. This discrepancy might be due to the different purification procedures for ubiquitylated tau and/or the different tau cDNA used. Shimura *et al.* (2003) used EGFP-tagged tau. As recombinant tau, which was not phosphorylated, could be ubiquitylated in an *in vitro* reconstitution system, CHIP must recognize and ubiquitylate both non-phospho and phospho tau.

The ubiquitinated tau found in AD brains was recovered in the SDS-insoluble fraction, suggesting that its ubiquitylation may precede fibril formation. A large amount of SDS-insoluble tau was recovered in P301L mutant tau-expressing cells in the present study and MG132 treatment enhanced the accumulation of tau in the SDS-insoluble fraction, suggesting that tau (P301L) is degraded by the ubiquitin–proteasome system. CHIP overexpression reduced the recovery of tau in the SDS-insoluble fraction and MG132 treatment showed only a small increase of SDS-insoluble tau, suggesting that the ubiquitylation of tau occurs before tau acquires insolubility against SDS. An inhibition of proteasome activity in the AD brain has been reported previously (Goldbaum *et al.* 2003; Keck *et al.* 2003). Taken together with the MG132-induced cytotoxicity of P301L tau overexpression, these results suggest that tau accumulation in the SDS-insoluble fraction itself was not toxic but rather that the neurons exhibited vulnerability against the stress of protein accumulation by inhibition of proteasome. CHIP expression reduces the stress induced by this cytotoxicity by reducing the amount of SDS-insoluble tau. Therefore, although CHIP-expressing neurons survive, ubiquitynated tau might remain in some neurons and develop into NFTs.

Acknowledgements

We thank S. Matsushita, K. Shinohara, N. Nishimura, R. Yasukouchi and other laboratory members for technical assistance and C. Sugita and M. Kimura for help in preparing the manuscript. This work was supported in part by a grant from the Ministry of Education, Science, Sports and Culture of Japan and by YASUDA Medical Research Foundation (SH).

References

Ballinger C. A., Connell P., Wu Y., Hu Z., Thompson L. J., Yin L. Y. and Patterson C. (1999) Identification of CHIP, a novel tetratricopeptide repeat-containing protein that interacts with heat shock proteins and negatively regulates chaperone functions. *Mol. Cell. Biol.* **19**, 4535–4545.

Connell P., Ballinger C. A., Jiang J., Wu Y., Thompson L. J., Hohfeld J. and Patterson C. (2001) The co-chaperone CHIP regulates protein triage decisions mediated by heat-shock proteins. *Nat. Cell Biol.* **3**, 93–96.

Dou F., Netzer W. J., Tanemura K., Li F., Hartl F. U., Takashima A., Gouras G. K., Greengard P. and Xu H. (2003) Chaperones increase association of tau protein with microtubules. *Proc. Natl Acad. Sci. USA* **100**, 721–726.

Goedert M., Hasegawa M., Jakes R., Lawler S., Cuenda A. and Cohen P. (1997) Phosphorylation of microtubule-associated protein tau by stress-activated protein kinases. *FEBS Lett.* **409**, 57–62.

Goldbaum O., Oppermann M., Handschuh M., Dabir D., Zhang B., Forman M. S., Trojanowski J. Q., Lee V. M. and Richter-Landsberg C. (2003) Proteasome inhibition stabilizes tau inclusions in oligodendroglial cells that occur after treatment with okadaic acid. *J. Neurosci.* **23**, 8872–8880.

Hardy J. and Selkoe D. J. (2002) The amyloid hypothesis of Alzheimer's disease: progress and problems on the road to therapeutics. *Science* **297**, 353–356.

Hatakeyama S. and Nakayama K. I. (2003) U-box proteins as a new family of ubiquitin ligases. *Biochem. Biophys. Res. Commun.* **302**, 635–645.

Hatakeyama S., Yada M., Matsumoto M., Ishida N. and Nakayama K. I. (2001) U box proteins as a new family of ubiquitin-protein ligases. *J. Biol. Chem.* **276**, 33 111–33 120.

Hershko A. (1983) Ubiquitin: roles in protein modification and breakdown. *Cell* **34**, 11–12.

Imai Y., Soda M., Hatakeyama S., Akagi T., Hashikawa T., Nakayama K. and Takahashi R. (2002) CHIP is associated with Parkin, a gene responsible for familial Parkinson's disease, and enhances its ubiquitin ligase activity. *Mol. Cell* **10**, 55–67.

Ishiguro K., Shiratsuchi A., Sato S., Omori A., Arioka M., Kobayashi S., Uchida T. and Imahori K. (1993) Glycogen synthase kinase 3 beta is identical to tau protein kinase I generating several epitopes of paired helical filaments. *FEBS Lett.* **325**, 167–172.

Keck S., Nitsch R., Grune T. and Ullrich O. (2003) Proteasome inhibition by paired helical filament-tau in brains of patients with Alzheimer's disease. *J. Neurochem.* **85**, 115–122.

Kopito R. R. and Ron D. (2000) Conformational disease. *Nat. Cell Biol.* **2**, E207–E209.

Lee V. M., Goedert M. and Trojanowski J. Q. (2001) Neurodegenerative tauopathies. *Annu. Rev. Neurosci.* **24**, 1121–1159.

Meacham G. C., Patterson C., Zhang W., Younger J. M. and Cyr D. M. (2001) The Hsc70 co-chaperone CHIP targets immature CFTR for proteasomal degradation. *Nat. Cell Biol.* **3**, 100–105.

Mori H., Kondo J. and Ihara Y. (1987) Ubiquitin is a component of paired helical filaments in Alzheimer's disease. *Science* **235**, 1641–1644.

Morishima-Kawashima M., Hasegawa M., Takio K., Suzuki M., Yoshida H., Titani K. and Ihara Y. (1995) Proline-directed and non-proline-directed phosphorylation of PHF-tau. *J. Biol. Chem.* **270**, 823–829.

Sato S., Tatebayashi Y., Akagi T. *et al.* (2002) Aberrant tau phosphorylation by glycogen synthase kinase-3beta and JNK3 induces oligomeric tau fibrils in COS-7 cells. *J. Biol. Chem.* **277**, 42 060–42 065.

Selkoe D. J. (2000) Toward a comprehensive theory for Alzheimer's disease. Hypothesis: Alzheimer's disease is caused by the cerebral accumulation and cytotoxicity of amyloid beta-protein. *Ann. NY Acad. Sci.* **924**, 17–25.

Shimura H., Schwartz D., Gygi S. P. and Kosik K. S. (2004) CHIP-Hsc70 complex ubiquitinates phosphorylated Tau and enhances cell survival. *J. Biol. Chem.* **279**, 4869–4876.

Tanemura K., Akagi T., Murayama M. *et al.* (2001) Formation of filamentous tau aggregations in transgenic mice expressing V337M human tau. *Neurobiol. Dis.* **8**, 1036–1045.

Tanemura K., Murayama M., Akagi T., Hashikawa T., Tominaga T., Ichikawa M., Yamaguchi H. and Takashima A. (2002) Neurode-

generation with tau accumulation in a transgenic mouse expressing V337M human tau. *J. Neurosci.* **22**, 133–141.

Tatebayashi Y., Miyasaka T., Chui D. H. *et al.* (2002) Tau filament formation and associative memory deficit in aged mice expressing mutant (R406W) human tau. *Proc. Natl Acad. Sci. USA* **99**, 13 896–13 901.

Weissman A. M. (2001) Themes and variations on ubiquitylation. *Nat. Rev. Mol. Cell Biol.* **2**, 169–178.

Xu W., Marcu M., Yuan X., Mimnaugh E., Patterson C. and Neckers L. (2002) Chaperone-dependent E3 ubiquitin ligase CHIP mediates a degradative pathway for c-ErbB2/Neu. *Proc. Natl Acad. Sci. USA* **99**, 12 847–12 852.

ELSEVIER

How do Parkin mutations result in neurodegeneration?

Yuzuru Imai and Ryosuke Takahashi

The gene product responsible for autosomal recessive juvenile Parkinsonism, Parkin, has been observed to have ubiquitin ligase activity. This finding has changed the direction of studies on Parkinson's disease by suggesting that abnormal protein turnover might be involved in its pathogenesis. A number of potentially neurotoxic Parkin-specific substrates have been identified. Further investigation of Parkin knockout mice will hopefully provide new evidence in the search for Parkin's substrates and further clarify their role in Parkinson's disease.

Addresses
Motor System Neurodegeneration, *RIKEN Brain Science Institute (BSI)*, Saitama 351-0198, Japan
e-mail: ryosuke@brain.riken.jp

Current Opinion in Neurobiology 2004, 14:384–389

This review comes from a themed issue on
Signalling mechanisms
Edited by Richard L Huganir and S Lawrence Zipursky

Available online 30th April 2004

0959-4388/$ – see front matter

DOI 10.1016/j.conb.2004.04.002

Abbreviations

AR-JP	*autosomal recessive juvenile* Parkinsonism
CDCrel-1	cell division control-related protein 1
CHIP	carboxy-terminus of Hsc70-interacting protein
E3	ubiquitin ligase
Hsp	heat shock protein
LB	Lewy body
Pael-R	Pael receptor
PD	Parkinson's disease
RING	really interesting new gene
TH	tyrosine hydroxylase
Ubl	ubiquitin-like domain

Introduction

Parkinson's disease (PD) is a movement disorder characterized by a progressive loss of dopaminergic neurons in the substantia nigra pars compacta. As in most cases of PD the degeneration is idiopathic, the etiology of the disease remains unknown. The recent identification of genetic mutations in familial cases of PD has advanced our understanding of the molecular mechanisms that cause the neurodegeneration.

Two rare missense mutations in the α-synuclein gene (A53T and A30P) cause autosomal dominant familial PD [1,2]. Although the physiological function of α-synuclein is still unclear, there is evidence that even wild type α-synuclein is a major component of Lewy bodies (LBs) and that its over-expression and gene triplication can cause neurodegeneration, which suggests that α-synuclein might play a part in the pathogenesis of PD [3,4]. LBs are intracytoplasmic eosinophilic inclusions composed of a core of granular and filamentous material surrounded by radiating filaments 10–15 nm in diameter. They are frequently found in affected neurons, including those of the substantia nigra, in the brains of patients with typical PD. This strongly suggests that there is an abnormality of protein turnover in PD.

Autosomal recessive juvenile Parkinsonism (AR-JP) is the most frequent form of familial PD. Mutations in the *parkin* gene were originally discovered from the linkage study of Japanese AR-JP families in 1998 [5]. Thereafter its mutations have been found worldwide. In patients with AR-JP, loss of dopaminergic neurons and consequently parkinsonian symptoms mostly occur without LB formation [6]. It has been demonstrated that wild type Parkin has ubiquitin ligase (E3) activity and that AR-JP-related mutant Parkin proteins do not [7–9]. Here, we discuss the recent studies on the physiological and pathophysiological role of Parkin.

Parkin as a ubiquitin ligase and its co-factors

Parkin has a ubiquitin-like domain (Ubl) at its amino-terminus and two really interesting new gene (RING) fingers flanking a cysteine-rich domain, known as the in between RING fingers (IBR) region (Figure 1). Several studies have recently revealed that numerous proteins with RING finger motifs have ubiquitin-protein ligase activity, which functions by itself or forms a complex with other components. An F-box (the name was given from a conserved motif originally found in cyclin F) protein with WD (Trp-Asp) repeats, hSel-10, and cullin-1 (one of cullin/CDC53 family members) have been shown to complex with Parkin, thus forming a SCF-like (named after their main components, Skp1, Cullin, and an F-box protein) E3 complex, which is involved in the degradation of cyclin E [10]. The authors of this report have suggested that, under normal circumstances, Parkin might regulate cyclin activity, and that neurodegeneration might occur in PD because of a disruption of this process. Parkin is also associated with the molecular chaperone heat shock protein 70 (Hsp 70), as well as another E3 carboxy-terminus of Hsc70-interacting protein (CHIP) [11,12]. CHIP, which was originally reported as an Hsc/Hsp70-binding protein, functions as a quality control monitor of proteins through its E3 function [13]. Recognition of abnormal proteins by Hsp70 and subsequent ubiquitination by CHIP support the regulation of quality control of intracellular proteins.

Figure 1

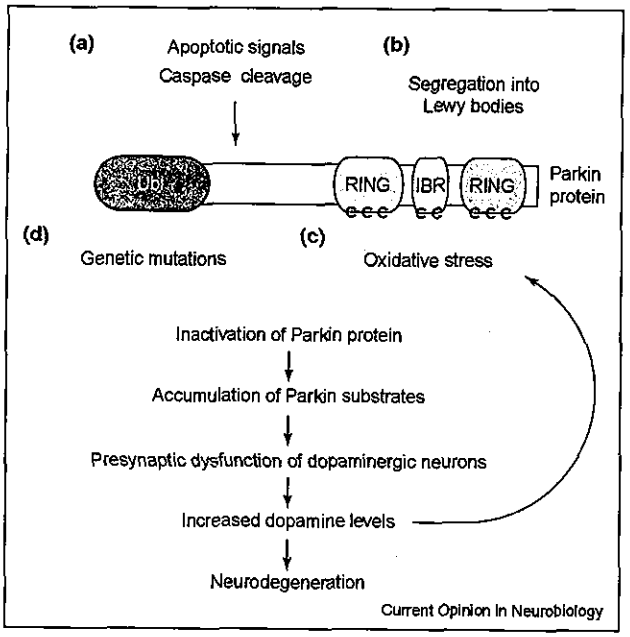

Proposed hypothesis of Parkin inactivation and subsequent neurodegeneration based on recent findings. The function of Parkin can be disturbed by four different factors. **(a)** Extracellular stress, inflammation, and insufficient neurotrophic factors can activate caspases that degrade Parkin [33,34]. **(b)** Protein inclusions, such as LBs, resulting from impairment of proteasome activity might sequester Parkin thereby eliminating its activity, although there is discrepancy among the results of immunostaining in LBs with different Parkin antibodies [17,30,31,39•]. **(c)** Oxidative stress within dopaminergic neurons has been suspected to be involved in PD, as an accumulation of iron is frequently observed in areas of degeneration in PD. Reactive oxidants, as well as dopamine/dopa-quinones, might modify a cluster of cysteine residues (represented by 'C') responsible for the E3 activity of Parkin, thus resulting in the precipitation of Parkin [22•,23]. Increased levels of intracellular dopamine and dopamine metabolites due to inactivation of Parkin might further perpetuate adduct formation with the cysteine residues of Parkin [42••,43•]. **(d)** Genetic mutations of the *parkin* gene, among other factors, might disturb Parkin function, resulting in an accumulation of Parkin substrates and subsequent neurodegeneration. The substrates of mammalian Parkin might differ from those of fly Parkin, such that a deficiency of Parkin might have different effects in the two species [25•].

As Parkin also ubiquitinates polyglutamine proteins through an Hsp70-mediated interaction, it is possible that Parkin functions in the same way as CHIP in degrading certain aberrant proteins through E3 activity after binding to Hsp70 [12]. In addition, CHIP co-operates with Parkin in the ubiquitination reaction responsible for endoplasmic reticulum-associated degradation (ERAD) [11].

Parkin substrates

There are a growing number of studies that report the identity of proteins that are ubiquitinated by Parkin (Table 1). Here, we feature four proteins out of Parkin's putative substrates. Cell division control-related protein 1 (CDCrel-1), which belongs to the Septin GTPase family, was the first reported Parkin substrate [9]. Although CDCrel-1 is thought to regulate neurotransmitter exocytosis, central nervous system abnormalities have not been detected in CDCrel-1-deficient mice. Specifically, alterations in synaptic firing have not been observed [14]. By contrast, over-expression of CDCrel-1 delivered by a viral vector induces dopamine-dependent neurodegeneration in the rodent brain [15•]. Another putative substrate of Parkin, the Pael receptor (Pael-R), which is a G protein-coupled orphan receptor, is abundantly expressed in dopaminergic neurons in the substantia nigra and tends to unfold even in a physiological condition. Thus, there is a possibility that excessive levels of unfolded Pael-R might lead to neuronal death as a result of unfolded protein stress. When Pael-R was expressed in all the neurons of the brain in *Drosophila melanogaster*, selective neurodegeneration of dopaminergic neurons was observed over time [16•]. Recently, immunolocalisation techniques have revealed Peal-R presence in Lewy bodies [17]. The p38 subunit of the aminoacyl-tRNA synthetase (ARS) complex is also ubiquitinated by Parkin [18]. The p38 subunit has been identified with immunolabelling in LBs in idiopathic cases of PD, whereas the ARS complex including the p38 subunit has been associated with protein biogenesis in a number of tissues as well as the brain [18]. It is believed that Synaptotagmin XI is localized with the secretory granules of neurotransmitters and plays a part in exocytosis stimulated by calcium ions. Synaptotagmin XI, which has been immunolabelled in LBs as well as normal neurons in the substantia nigra, is ubiquitinated and degraded in a Parkin-dependent manner [19]. Parkin inactivation causes a failure of Synaptotagmin XI to be ubiquitinated, and it is possible that this accounts for the disorder of dopamine release that is seen in Parkin-deficient mice.

Parkin and α-synuclein

A number of investigators in this field question whether or not there is a relationship between *parkin* and *α-synuclein*, as mutations of both these genes are causative of familial PD. Some studies have shown Parkin to attenuate wild type or mutant α-synuclein-mediated neurotoxicity within tyrosine hydroxylase (TH)-positive neurons, however, Parkin has not been observed to ubiquitinate α-synuclein *in vitro*. When mutant α-synuclein escapes the regulation of quality control of intracellular proteins, it sensitizes catecholaminergic neurons and impairs proteasomal activity [20]. Over-expression of Parkin rescues TH-positive cells from mutant α-synuclein toxicity and the effects of proteasomal inhibition [20,21]. Similar results have been observed in TH-positive *Drosophila* neurons [16•]. Now that Parkin-deficient mice can be used as a model, the genetic link between these two genes, as well as other genes involved in familial cases of PD, can be investigated in mammals.

Table 1

Reported substrates of Parkin.

Protein	Physiological or pathological function	Immunopositivity detected in LBs	Methods of identification	References
CDCrel-1	Septin family protein with unknown function	–	Y	[9,44]
O-glycosylated α-synuclein	Isoform of α-synuclein with unknown function	N.D.	I	[45]
Pael receptor	Orphan G-protein coupled receptor	+	Y	[17,46]
p38 subunit of the aminoacyl-tRNA synthetase	Role in protein biosynthesis	+	Y	[18]
Synaptotagmin XI	Regulates exocytosis of neurotransmitters	+	Y	[19]
Expanded polyglutamine(polyQ) proteins	Aberrant proteins responsible for polyQ diseases	N.D.	I	[12]
α/β-tubulins	Microtubule proteins	+	I	[47,48]
Synphilin-1	α-synuclein-binding protein	+	I	[49,50]
Cyclin E	Cell cycle regulation of mitotic cells; unknown function in neurons	N.D.	I	[10]
SEPT5_v2/CDCrel-2	SEPT5_v2 is highly homologous with CDCrel-1	N.D.	Y	[51]

Common features or binding motifs have not been identified among these reported substrates of Parkin. Some of them have been observed within LBs or Lewy neuritis ('+' and '–' mean immunopositive and immunonegative, respectively, 'N.D.' indicates not determined). This finding suggests that Parkin dysfunction might be involved in some part of PD as well as AR-JP. 'Y' and 'I' in methods of identification indicate yeast two-hybrid screening and immunoprecipitation (or pull-down)/western blot assay, respectively.

The role of Parkin against stress

Oxidative stress is thought to play a part in neurodegeneration. As the cysteine residues of Parkin are integral to its E3 activity, alteration of these residues by reactive materials, such as an oxygen radical, might impair the function of Parkin. Indeed, peroxide has been shown to generate mis-folded Parkin [22•]. In addition, the three amino acids at the carboxy-terminal of Parkin are necessary for proper folding and probably its function, such that a pathogenic mutant, known as W453Stop, fails to adopt the native conformation of Parkin. Interestingly, induction of chaperones by heat shock reduces the mis-folding of Parkin that occurs following treatment with peroxide. One Parkin-binding protein, Hsp70, along with its co-chaperone, Hsp40, has been observed to inhibit partially the precipitation of both peroxide-treated and mutant Parkin *in vitro*, although recovery of Parkin's E3 activity has not been observed. The results of another study suggest that impairment of proteasomal activity by stable expression of Parkin mutants leads to accumulation of damaged proteins and lipids due to oxidation, thus sensitizing neurons to various forms of stress, which results in neuronal death [23].

Over-expression of Parkin has been observed to attenuate C2-ceramide-mediated mitochondrial swelling prior to cell death [24]. Subcellular fractionation experiments have revealed substantial amounts of Parkin on the outer mitochondrial membrane, however, the mechanism by which over-expression of Parkin might protect mitochondrial integrity is unknown as yet. The only orthologous gene of human *parkin* has been discovered in the *Drosophila* genome. This gene product has 59% overall similarity with human Parkin. Notably, *Drosophila parkin* null mutants have been found to exhibit markedly different pathology than that observed in human cases of PD [25•]. Specifically, evidence of degeneration of TH-positive neurons in the brains of *Drosophila parkin* null mutants is lacking. The mechanisms behind the remarkable phenotypic differences between Parkin deficient humans and flies are still unknown, although there is a possibility that the *Drosophila* ortholog recognizes a fly-specific substrate(s), which is not associated with AR-JP. Importantly, it has been observed that mitochondrial dysfunction in some muscles and spermatids that undergo high energy metabolism can be reversed upon transgenic expression of *Drosophila* Parkin. These findings indicate that Parkin might maintain mitochondrial function even in humans, thereby protecting cells from the oxidative stress that is generated by mitochondrial dysfunction.

Ubl-containing proteins, such as Rad23 and Dsk2, interact with the 26S proteasome through the Ubl, thus linking the 26S proteasome to ubiquitination enzymes. The Ubl of Parkin has a typical ubiquitin fold and binds to Rpn10, Rnt6 and C3, all of which are subunits of proteasome complexes [12,26•,27,28]. In addition, binding between Parkin and various proteasome complexes appears to be ATP-dependent [11]. The results of another study suggest that the Ubl might function as an unstable tag for breakdown despite the lack of necessity for Parkin auto-ubiquitination, thereby regulating the level of cellular Parkin [29]. Mutations affecting Ubl function have been identified in both humans (R42P) and *Drosophila* (A46T) with neurodegeneration in human and mitochondrial dysfunction in *Drosophila*, thus indicating the importance of the Ubl domain for Parkin function. A number of investigators have frequently observed processing of Parkin around the end of its Ubl domain [10,20,22•,30–32]. Some of the enzymes involved in this processing were shown to be caspases, which suggests that apoptotic signaling following various forms of cell stress inactivates the

Parkin protein [33,34]. This idea is supported by the finding of an absence of Parkin following cerebral injury due to transient ischemia, and a subsequent reduction in ATP levels [35]. Although several lines of evidence suggest that up-regulation of Parkin enhances its protective function against unfolded protein stress, inconsistent observations imply the involvement of cell-type specific factors in the regulation of the *parkin* gene [7,35,36]. Astrocytes, which express lower levels of Parkin than hippocampal neurons, have a propensity to induce Parkin expression and subcellular redistribution of Parkin during unfolded protein stress, whereas hippocampal neurons do not [37]. This observation might partially explain why dopaminergic neurons as well as other neurons are especially vulnerable to any stress caused by generation of unfolded proteins.

Parkin in cellular protein inclusions and Lewy bodies

LBs are a pathological hallmark of PD. The presence of LBs in affected regions, among others, in PD indicates that improper handling of proteins might be involved pathogenesis of the disease. However, the mechanism by which LBs are formed and their role in neurodegeneration remain unknown. Neurodegeneration in AR-JP is not accompanied by obvious LB formation. By contrast, it has been demonstrated that both isolated LBs and LBs in paraffin sections are immunopositive for Parkin [17,31]. Protein inclusions, such as aggresomes, can be experimentally induced by proteasomal inhibition in both neuronal and non-neuronal cells. Considerable immunocytochemical analyses have reported that Parkin, as well as a number of other proteins within LBs, is localized in the cellular inclusions following exposure of cells to proteasome inhibitors [32,38,39•,40,41]. This suggests that LBs and other cellular protein inclusions could work to isolate Parkin, thereby eliminating its function. This idea raises the possibility that sequestering of Parkin is a factor contributing to neurodegeneration even in idiopathic PD with LBs. By contrast, a series of immunohistochemical experiments using different monoclonal and polyclonal antibodies to Parkin failed to detect Parkin-immunoreactivity in LBs [19,30]. Another immunocytochemical study has reported that endogenous Parkin in human dopaminergic neuroblastoma SH-SY5Y cells is recruited into perinuclear inclusions after treatment with dopamine and a pro-apoptotic reagent staurosporine, as well as a proteasome inhibitor [32]. Although transgenic over-expression of Parkin suppresses cellular inclusions induced by these kinds of stress, the inhibition of inclusion formation by Parkin is not always associated with protection from cell death [32].

Animal models of AR-JP

The first reports of experiments conducted with Parkin-deficient mice come from two different research groups [42••,43•]. Although a macroscopic loss of nigrostriatal dopaminergic neurons has not been reported, evidence of pre-synaptic dysfunction of dopaminergic and glutamatergic neurons has been found in association with altered behavior that could be caused by neuronal dysfunctions. Remarkably, it has been observed that Parkin-deficient mice have increased levels of dopamine and dopamine metabolites within their striatum. These phenomena suggest that Parkin is necessary for maintenance of the synaptic functions in dopaminergic neurons as well as other neurons.

Conclusions

The ubiquitin system plays a part in the sorting of membrane proteins, endocytosis of receptors at the plasma membrane, transactivation of genes, and protein degradation. However, several lines of evidence suggest that Parkin takes a role in protein degradation through binding of its Ubl to the proteasomes. The recent development of Parkin-deficient mice will help to confirm whether or not accumulation of proposed substrates of Parkin is responsible for neurodegeneration, as well as to assist in the identification of novel substrates, thus shedding light on the pathogenesis of AR-JP (Figure 1). For example, by crossbreeding mice it will be possible to analyse genetic interactions of Parkin and its substrates with the hope of finding a true substrate responsible for AR-JP, which will be the first step to the next generation of PD study.

Acknowledgements

Work in our laboratory was partially supported by the Ministry of education, Science, Sports and Culture, Grant-in-Aid for Scientific research on Priority areas, Advanced Brain Science Project #15016120 and Scientific Research (A) #14207032 to R Takahashi. Young Scientists (A) #15680011 and a grant from Special Postdoctoral Researcher of RIKEN to Y Imai.

References and recommended reading

Papers of particular interest, published within the annual period of review, have been highlighted as:

- • of special interest
- •• of outstanding interest

1. Polymeropoulos MH, Lavedan C, Leroy E, Ide SE, Dehejia A, Dutra A, Pike B, Root H, Rubenstein J, Boyer R *et al.*: **Mutation in the alpha-synuclein gene identified in families with Parkinson's disease.** *Science* 1997, **276**:2045-2047.

2. Krüger R, Kuhn W, Müller T, Woitalla D, Graeber M, Kosel S, Przuntek H, Epplen JT, Schols L, Riess O: **Ala30Pro mutation in the gene encoding alpha-synuclein in Parkinson's disease.** *Nat Genet* 1998, **18**:106-108.

3. Trojanowski JQ, Goedert M, Iwatsubo T, Lee VM: **Fatal attractions: abnormal protein aggregation and neuron death in Parkinson's disease and Lewy body dementia.** *Cell Death Differ* 1998, **5**:832-837.

4. Singleton AB, Farrer M, Johnson J, Singleton A, Hague S, Kachergus J, Hulihan M, Peuralinna T, Dutra A, Nussbaum R *et al.*: **Alpha-synuclein locus triplication causes Parkinson's disease.** *Science* 2003, **302**:841.

5. Kitada T, Asakawa S, Hattori N, Matsumine H, Yamamura Y, Minoshima S, Yokochi M, Mizuno Y, Shimizu N: **Mutations in the parkin gene cause autosomal recessive juvenile parkinsonism.** *Nature* 1998, **392**:605-608.

6. Mizuno Y, Hattori N, Matsumine H: **Neurochemical and neurogenetic correlates of Parkinson's disease.** *J Neurochem* 1998, **71**:893-902.

7. Imai Y, Soda M, Takahashi R: **Parkin suppresses unfolded protein stress-induced cell death through its E3 ubiquitin-protein ligase activity.** *J Biol Chem* 2000, **275**:35661-35664.

8. Shimura H, Hattori N, Kubo S, Mizuno Y, Asakawa S, Minoshima S, Shimizu N, Iwai K, Chiba T, Tanaka K *et al.*: **Familial Parkinson disease gene product, Parkin, is a ubiquitin-protein ligase.** *Nat Genet* 2000, **25**:302-305.

9. Zhang Y, Gao J, Chung KK, Huang H, Dawson VL, Dawson TM: **Parkin functions as an E2-dependent ubiquitin- protein ligase and promotes the degradation of the synaptic vesicle-associated protein, CDCrel-1.** *Proc Natl Acad Sci USA* 2000, **97**:13354-13359.

10. Staropoli JF, McDermott C, Martinat C, Schulman B, Demireva E, Abeliovich A: **Parkin is a component of an SCF-like ubiquitin ligase complex and protects postmitotic neurons from kainate excitotoxicity.** *Neuron* 2003, **37**:735-749.

11. Imai Y, Soda M, Hatakeyama S, Akagi T, Hashikawa T, Nakayama KI, Takahashi R: **CHIP is associated with Parkin, a gene responsible for familial Parkinson's disease, and enhances its ubiquitin ligase activity.** *Mol Cell* 2002, **10**:55-67.

12. Tsai YC, Fishman PS, Thakor NV, Oyler GA: **Parkin facilitates the elimination of expanded polyglutamine proteins and leads to preservation of proteasome function.** *J Biol Chem* 2003, **278**:22044-22055.

13. Murata S, Minami Y, Minami M, Chiba T, Tanaka K: **CHIP is a chaperone-dependent E3 ligase that ubiquitylates unfolded protein.** *EMBO Rep* 2001, **2**:1133-1138.

14. Peng XR, Jia Z, Zhang Y, Ware J, Trimble WS: **The septin CDCrel-1 is dispensable for normal development and neurotransmitter release.** *Mol Cell Biol* 2002, **22**:378-387.

15. • Dong Z, Ferger B, Paterna JC, Vogel D, Furler S, Osinde M, Feldon J, Bueler H: **Dopamine-dependent neurodegeneration in rats induced by viral vector-mediated overexpression of the Parkin target protein, CDCrel-1.** *Proc Natl Acad Sci USA* 2003, **100**:12438-12443.

This *in vivo* study using a recombinant adeno-associated virus shows that CDCrel-1 over-expression in nigrostriatal regions induces selective degeneration of TH-positive neurons, which can be prevented by inhibition of dopamine synthesis.

16. • Yang Y, Nishimura I, Imai Y, Takahashi R, Lu B: **Parkin suppresses dopaminergic neuron-selective neurotoxicity induced by Pael-R in *Drosophila*.** *Neuron* 2003, **37**:911-924.

The authors demonstrate that Pael-R overexpression in the fly brain results in the elimination of TH-positive neurons but not other neurons, which is enhanced by Parkin knockdown using RNA interference. This result, together with that of Dong *et al.* [15•], suggests that a common mechanism underlies the degeneration of TH-positive neurons by over-expression of CDCrel-1 or Pael-R, and that dopamine and dopamine metabolites are involved in this process. They also show that Parkin overexpression suppresses α-synuclein neurotoxicity in the fly brain.

17. Murakami T, Shoji M, Imai Y, Inoue H, Kawarabayashi T, Matsubara E, Harigaya Y, Sasaki A, Takahashi R, Abe K: **Pael-R is accumulated in Lewy bodies of Parkinson's disease.** *Ann Neurol* 2004, **55**:439-442.

18. Corti O, Hampe C, Koutnikova H, Darios F, Jacquier S, Prigent A, Robinson JC, Pradier L, Ruberg M, Mirande M *et al.*: **The p38 subunit of the aminoacyl-tRNA synthetase complex is a Parkin substrate: linking protein biosynthesis and neurodegeneration.** *Hum Mol Genet* 2003, **12**:1427-1437.

19. Huynh DP, Scoles DR, Nguyen D, Pulst SM: **The autosomal recessive juvenile Parkinson disease gene product, Parkin, interacts with and ubiquitinates synaptotagmin XI.** *Hum Mol Genet* 2003, **12**:2587-2597.

20. Petrucelli L, O'Farrell C, Lockhart PJ, Baptista M, Kehoe K, Vink L, Choi P, Wolozin B, Farrer M, Hardy J *et al.*: **Parkin protects against the toxicity associated with mutant alpha-synuclein: proteasome dysfunction selectively affects catecholaminergic neurons.** *Neuron* 2002, **36**:1007-1019.

21. Oluwatosin-Chigbu Y, Robbins A, Scott CW, Arriza JL, Reid JD, Zysk JR: **Parkin suppresses wild-type alpha-synuclein-induced toxicity in SHSY-5Y cells.** *Biochem Biophys Res Commun* 2003, **309**:679-684.

22. • Winklhofer KF, Henn IH, Kay-Jackson PC, Heller U, Tatzelt J: **Inactivation of Parkin by oxidative stress and C-terminal truncations: a protective role of molecular chaperones.** *J Biol Chem* 2003, **278**:47199-47208.

This study suggests the possibility that oxidative stress inactivates Parkin. Treatment of Parkin-expressing cells with thermal and oxidative stress promotes the formation of 0.1% triton X-100-insoluble Parkin protein, a phenomenon that is suppressed by the induction of heat shock chaperones.

23. Hyun DH, Lee M, Hattori N, Kubo S, Mizuno Y, Halliwell B, Jenner P: **Effect of wild-type or mutant Parkin on oxidative damage, nitric oxide, antioxidant defences, and the proteasome.** *J Biol Chem* 2002, **277**:28572-28577.

24. Darios F, Corti O, Lucking CB, Hampe C, Muriel MP, Abbas N, Gu WJ, Hirsch EC, Rooney T, Ruberg M *et al.*: **Parkin prevents mitochondrial swelling and cytochrome c release in mitochondria-dependent cell death.** *Hum Mol Genet* 2003, **12**:517-526.

25. • Greene JC, Whitworth AJ, Kuo I, Andrews LA, Feany MB, Pallanck LJ: **Mitochondrial pathology and apoptotic muscle degeneration in *Drosophila parkin* mutants.** *Proc Natl Acad Sci USA* 2003, **100**:4078-4083.

This is the first report of a Parkin-deficient animal. The authors created several lines of *Drosophila parkin* null mutants so these mutants exhibit a more severe phenotype caused by mitochondria dysfunction rather than pathology of AR-JP. However, degeneration of TH-positive neurons was not observed.

26. • Sakata E, Yamaguchi Y, Kurimoto E, Kikuchi J, Yokoyama S, Yamada S, Kawahara H, Yokosawa H, Hattori N, Mizuno Y *et al.*: **Parkin binds the Rpn10 subunit of 26S proteasomes through its ubiquitin-like domain.** *EMBO Rep* 2003, **4**:301-306.

This structural study, together with the nuclear magnetic resonance (NMR) study of Tashiro *et al.* [27], reveals that the Ubl of Parkin has a typical ubiquitin fold. This study also shows that the arginine residue at amino-acid position 42 within the Ubl, where an AR-JP-related single mutation (R42P) has been found, contributes to the interaction with a subunit of the 26S proteasome, which provides strong evidence for the involvement of Parkin in protein breakdown.

27. Tashiro M, Okubo S, Shimotakahara S, Hatanaka H, Yasuda H, Kainosho M, Yokoyama S, Shindo H: **NMR structure of ubiquitin-like domain in Parkin: gene product of familial Parkinson's disease.** *J Biomol NMR* 2003, **25**:153-156.

28. Upadhya SC, Hegde AN: **A potential proteasome-interacting motif within the ubiquitin-like domain of Parkin and other proteins.** *Trends Biochem Sci* 2003, **28**:280-283.

29. Finney N, Walther F, Mantel PY, Stauffer D, Rovelli G, Dev KK: **The cellular protein level of Parkin is regulated by its ubiquitin-like domain.** *J Biol Chem* 2003, **278**:16054-16058.

30. Pawlyk AC, Giasson BI, Sampathu DM, Perez FA, Lim KL, Dawson VL, Dawson TM, Palmiter RD, Trojanowski JQ, Lee VM: **Novel monoclonal antibodies demonstrate biochemical variation of brain Parkin with age.** *J Biol Chem* 2003, **278**:48120-48128.

31. Schlossmacher MG, Frosch MP, Gai WP, Medina M, Sharma N, Forno L, Ochiishi T, Shimura H, Sharon R, Hattori N *et al.*: **Parkin localizes to the Lewy bodies of Parkinson's disease and dementia with Lewy bodies.** *Am J Pathol* 2002, **160**:1655-1667.

32. Muqit MM, Davidson SM, Payne Smith MD, MacCormac LP, Kahns S, Jensen PH, Wood NW, Latchman DS: **Parkin is recruited into aggresomes in a stress-specific manner: over-expression of Parkin reduces aggresome formation but can be dissociated from Parkin's effect on neuronal survival.** *Hum Mol Genet* 2004, **13**:117-135.

33. Kahns S, Lykkebo S, Jakobsen LD, Nielsen MS, Jensen PH: **Caspase-mediated Parkin cleavage in apoptotic cell death.** *J Biol Chem* 2002, **277**:15303-15308.

34. Kahns S, Kalai M, Jakobsen LD, Clark BF, Vandenabeele P, Jensen PH: **Caspase-1 and caspase-8 cleave and inactivate cellular Parkin.** *J Biol Chem* 2003, **278**:23376-23380.

35. Mengesdorf T, Jensen PH, Mies G, Aufenberg C, Paschen W: **Down-regulation of Parkin protein in transient focal cerebral ischemia: a link between stroke and degenerative disease?** *Proc Natl Acad Sci USA* 2002, **99**:15042-15047.

36. West AB, Gonzalez-de-Chavez F, Wilkes K, O'Farrell C, Farrer MJ: **Parkin is not regulated by the unfolded protein response in human neuroblastoma cells.** *Neurosci Lett* 2003, **341**:139-142.

37. Ledesma MD, Galvan C, Hellias B, Dotti C, Jensen PH: **Astrocytic but not neuronal increased expression and redistribution of Parkin during unfolded protein stress.** *J Neurochem* 2002, **83**:1431-1440.

38. Ardley HC, Scott GB, Rose SA, Tan NG, Markham AF, Robinson PA: **Inhibition of proteasomal activity causes inclusion formation in neuronal and non-neuronal cells overexpressing Parkin.** *Mol Biol Cell* 2003, **14**:4541-4556.

39. • Junn E, Lee SS, Suhr UT, Mouradian MM: **Parkin accumulation in aggresomes due to proteasome impairment.** *J Biol Chem* 2002, **277**:47870-47877.
This *in vitro* study of the effects of proteasome inhibitors shows that Parkin, as well as α-synuclein and other proteins within LBs, co-localizes within aggresomes in cultured cells. This result implies that aggresome formation is related to that of LBs in PD. The studies of Ardley *et al.* [38], Zhao *et al.* [40] and Imai *et al.* [41] give similar results.

40. Zhao J, Ren Y, Jiang Q, Feng J: **Parkin is recruited to the centrosome in response to inhibition of proteasomes.** *J Cell Sci* 2003, **116**:4011-4019.

41. Imai Y, Soda M, Murakami T, Shoji M, Abe K, Takahashi R: **A product of the human gene adjacent to parkin is a component of Lewy bodies and suppresses Pael receptor-induced cell death.** *J Biol Chem* 2003, **278**:51901-51910.

42. •• Itier JM, Ibáñez P, Mena MA, Abbas N, Cohen-Salmon C, Bohme GA, Laville M, Pratt J, Corti O, Pradier L *et al.*: **Parkin gene inactivation alters behaviour and dopamine neurotransmission in the mouse.** *Hum Mol Genet* 2003, **12**:2277-2291.
This paper is the first report of Parkin-deficient mice, in which the authors observed pre-synaptic dysfunction of neurons, along with an increase in dopamine and dopamine metabolites, and motor and cognitive deficits. However, neither this nor a subsequent report by Goldberg *et al.* [43•] observed macroscopic degeneration of dopaminergic neurons with age.

43. • Goldberg MS, Fleming SM, Palacino JJ, Cepeda C, Lam HA, Bhatnagar A, Meloni EG, Wu N, Ackerson LC, Klapstein GJ *et al.*: **Parkin-deficient mice exhibit nigrostriatal deficits but not loss of dopaminergic neurons.** *J Biol Chem* 2003, **278**:43628-43635.
This study shows an increase in extracellular dopamine within the striatum by microdialysis. Electrophysiological deficits in striatal neurons and motor deficits in Parkin-deficient mice are also demonstrated.

44. Ihara M, Tomimoto H, Kitayama H, Morioka Y, Akiguchi I, Shibasaki H, Noda M, Kinoshita M: **Association of the cytoskeletal GTP-binding protein Sept4/H5 with cytoplasmic inclusions found in Parkinson's disease and other synucleinopathies.** *J Biol Chem* 2003, **278**:24095-24102.

45. Shimura H, Schlossmacher MG, Hattori N, Frosch MP, Trockenbacher A, Schneider R, Mizuno Y, Kosik KS, Selkoe DJ: **Ubiquitination of a new form of alpha-synuclein by Parkin from human brain: implications for Parkinson's disease.** *Science* 2001, **293**:263-269.

46. Imai Y, Soda M, Inoue H, Hattori N, Mizuno Y, Takahashi R: **An unfolded putative transmembrane polypeptide, which can lead to endoplasmic reticulum stress, is a substrate of Parkin.** *Cell* 2001, **105**:891-902.

47. Ren Y, Zhao J, Feng J: **Parkin binds to alpha/beta tubulin and increases their ubiquitination and degradation.** *J Neurosci* 2003, **23**:3316-3324.

48. Iseki E, Marui W, Sawada H, Ueda K, Kosaka K: **Accumulation of human alpha-synuclein in different cytoskeletons in Lewy bodies in brains of dementia with Lewy bodies.** *Neurosci Lett* 2000, **290**:41-44.

49. Chung KK, Zhang Y, Lim KL, Tanaka Y, Huang H, Gao J, Ross CA, Dawson VL, Dawson TM: **Parkin ubiquitinates the alpha-synuclein-interacting protein, synphilin- 1: implications for Lewy-body formation in Parkinson's disease.** *Nat Med* 2001, **7**:1144-1150.

50. Wakabayashi K, Engelender S, Yoshimoto M, Tsuji S, Ross CA, Takahashi H: **Synphilin-1 is present in Lewy bodies in Parkinson's disease.** *Ann Neurol* 2000, **47**:521-523.

51. Choi P, Snyder H, Petrucelli L, Theisler C, Chong M, Zhang Y, Lim K, Chung KK, Kehoe K, D'Adamio L *et al.*: **SEPT5_v2 is a parkin-binding protein.** *Brain Res Mol Brain Res* 2003, **117**:179-189.

Superoxide Production at Phagosomal Cup/Phagosome through βI Protein Kinase C during FcγR-Mediated Phagocytosis in Microglia[1]

Takehiko Ueyama,* Michelle R. Lennartz,*† Yukiko Noda,‡ Toshihiro Kobayashi,§ Yasuhito Shirai,* Kyoko Rikitake,* Tomoko Yamasaki,‡ Shigeto Hayashi,* Norio Sakai,*¶ Harumichi Seguchi,§ Makoto Sawada,‖ Hideki Sumimoto,## and Naoaki Saito[2]*

Protein kinase C (PKC) plays a prominent role in immune signaling. To elucidate the signal transduction in a respiratory burst and isoform-specific function of PKC during FcγR-mediated phagocytosis, we used live, digital fluorescence imaging of mouse microglial cells expressing GFP-tagged molecules. βI PKC, εPKC, and diacylglycerol kinase (DGK) β dynamically and transiently accumulated around IgG-opsonized beads (BIgG). Moreover, the accumulation of $p47^{phox}$, an essential cytosolic component of NADPH oxidase and a substrate for βI PKC, at the phagosomal cup/phagosome was apparent during BIgG ingestion. Superoxide (O_2^-) production was profoundly inhibited by Gö6976, a cPKC inhibitor, and dramatically increased by the DGK inhibitor, R59949. Ultrastructural analysis revealed that BIgG induced O_2^- production at the phagosome but not at the intracellular granules. We conclude that activation/accumulation of βI PKC is involved in O_2^- production, and that O_2^- production is primarily initiated at the phagosomal cup/phagosome. This study also suggests that DGKβ plays a prominent role in regulation of O_2^- production during FcγR-mediated phagocytosis. *The Journal of Immunology*, 2004, 173: 4582–4589.

Microglia have been described as resident macrophages in the CNS. Invading pathogens are removed via phagocytosis using the Fcγ, complement, scavenger, mannose, phosphatidylserine, and TLR (1). Over the past few years, phagocytosis in microglia, especially FcγR-mediated phagocytosis, has attracted a great deal of attention in the context of potential therapy for Alzheimer's disease (2).

Protein kinase C (PKC)[3] comprises a family of 10 isoforms (3). The conventional isoforms (cPKC; α, βI, βII, and γ) are Ca^{2+} and diacylglycerol (DAG)-dependent, the novel isoforms (nPKC; δ, ε, η, and θ) are also DAG-dependent, but Ca^{2+} independent, and the atypical isoforms (ζ and ιλ) are nonresponsive to Ca^{2+} or DAG. Phenotypes for various PKC knockout mice have shown a role for a specific isoform in the immune system. Mice deficient in βPKC have a marked immunodeficiency (4), and show a reduced production of the superoxide (O_2^-), a precursor of microbicidal oxidants, during FcγR-mediated phagocytosis in neutrophils (5). In the absence of εPKC, host defense against bacterial infection is severely compromised (6). The signaling capacity of DAG can be terminated by its conversion to phosphatidic acid through the action of diacylglycerol kinase (DGK). DGK family is composed of nine mammalian subtypes and is grouped into five classes; type I DGK (α, β, and γ) has Ca^{2+}-binding motifs (7). Because excessive O_2^- production appears to be harmful to normal cells and tissues (8), it is implicated that O_2^- production involved in βPKC has a tight regulation by DGK isoform.

FcγR-mediated phagocytosis is a spatiotemporally regulated signaling cascade with two rapid responses, remodeling of the cytoskeleton and activation of the respiratory burst. Phospholipase C (PLC) γ, a key enzyme for actin remodeling, is activated upon engagement of FcγRs (9). DAG and inositol-1,4,5-triphosphate (IP_3) from PLCγ activation exert their effects by stimulating PKC or by changing intracellular Ca^{2+} concentration ($[Ca^{2+}]_i$), respectively. The respiratory burst is initiated by the phagocyte NADPH oxidase, which is dormant in resting cells, but becomes activated during phagocytosis to produce O_2^- (10). NADPH oxidase is a multiprotein complex that is assembled from a membrane-spanning cytochrome b_{558} ($gp91^{phox}$ and $p22^{phox}$) and four main cytosolic factors ($p47^{phox}$, $p67^{phox}$, $p40^{phox}$, and Rac) that translocate to the cytochrome b_{558} to generate the active enzyme. Various protein kinases, including PKC, MAPK, PKA, the p21-activated kinases, phosphatidic acid-regulated protein kinases, and Akt (protein kinase B) have been reported to activate NADPH oxidase through phosphorylation of $p47^{phox}$ (11, 12). In neutrophils stimulated by PMA, the intracellular granules are proposed as the initial O_2^--producing sites, then these granules fuse with the plasma

*Laboratory of Molecular Pharmacology, Biosignal Research Center, Kobe University, Kobe, Japan; †Center for Cell Biology and Cancer Research, Albany Medical College, Albany, NY 12208; §Department of Anatomy and Cell Biology, Kochi Medical School, Kochi, Japan; ‡Medical Institute of Bioregulation, Kyushu University, Fukuoka, Japan; ¶Graduate School of Biomedical Sciences, Hiroshima University, Hiroshima, Japan; ‖Institute for Comprehensive Medical Science, Fujita Health University, Toyoake, Japan; and ##CREST JST (Japan Science and Technology)

Received for publication April 5, 2004. Accepted for publication July 16, 2004.

The costs of publication of this article were defrayed in part by the payment of page charges. This article must therefore be hereby marked *advertisement* in accordance with 18 U.S.C. Section 1734 solely to indicate this fact.

[1] *This work was supported by grants from the 21st Century Center of Excellence Program of the Ministry of Education, Culture, Sports, Science, and Technology of Japan, Core Research for Evolutional Science and Technology, the Ministry of Education, Culture, Sports, Science, and Technology in Japan, a Grant-in-Aid for Scientific Research on Priority Areas (C)-Advanced Brain Science Project from the Ministry of Education, Culture, Sports, Science, and Technology in Japan, the Uehara Memorial Foundation, and the Sankyo Foundation of Life Science.*

[2] Address correspondence and reprint requests to Dr. Naoaki Saito, Laboratory of Molecular Pharmacology, Biosignal Research Center, Kobe University, Rokkodai-cho 1-1, Nada-ku, Kobe 657-8501, Japan. E-mail address: naosaito@kobe-u.ac.jp

[3] Abbreviations used in this paper: PKC, protein kinase C; DGK, diacylglycerol kinase; MARCKS, myristoylated alanine-rich C kinase substrate; c, conventional isoform; n, novel isoform; DAG, diacylglycerol; O_2^- superoxide; PLC, phospholipase C; IP_3, inositol-1,4,5-triphosphate; $[Ca^{2+}]_i$, intracellular Ca^{2+} concentration; BIgG, IgG-opsonized beads.

0022-1767/04/$02.00

membrane, resulting in the delivery of O_2^- into the extracellular milieu (13, 14). However, PMA is a nonphysiological stimulus and results obtained using PMA may not accurately reflect the cell response to a physiological stimulus.

We now face the challenge of defining 1) the PKC involved signal transduction pathway regulated by DGK, 2) the isoform-specific function of PKC, and 3) the intracellular site of O_2^- production, during a FcγR-mediated respiratory burst at the cellular level. Unfortunately, primary neutrophils have a severely limited lifetime ex vivo, and both primary and cultured neutrophils are difficult to be transfected. Monocytes have a markedly reduced capacity for O_2^- production compared with neutrophils. To overcome these problems, we used our microglial cells and visualized the accumulation of βI and εPKC, DGKβ and $p47^{phox}$ to the phagosome using real-time confocal laser scanning fluorescence microscopy. In this study, we show that βI PKC contributes to O_2^- production, and that DGKβ plays an important role in regulation of O_2^- production, probably in control of excessive O_2^- production. Finally, we demonstrate that the O_2^--producing site during FcγR-mediated phagocytosis is at the phagosomal cup/phagosome.

Materials and Methods

Reagents

Two-micrometer glass beads and carboxylated latex beads were obtained from Duke Scientific (Palo Alto, CA) and Polysciences (Warrington, PA), respectively. Eagle's MEM and endotoxin-free FBS were from Invitrogen Life Technologies (Carlsbad, CA). Bovine insulin and PMA were from Sigma-Aldrich (St. Louis, MO). Mouse GM-CSF was from Genzyme (Cambridge, MA). U73122 and U73343 were from Biomol (Plymouth Meeting, PA), and Gö6976 and R59949 were from Calbiochem (San Diego, CA). Fura 2-AM was from Dojindo (Kumamoto, Japan).

Cell culture

The 6-3 microglial cells are generated by spontaneous immortalization of primary microglia from *op/op* mice which are deficient of M-CSF-derived macrophages and severely monocytopenic (15, 16). The 6-3 cells closely resemble primary microglia with respect to microglia-specific gene expression and high migrating activity to the brain (15, 17). The 6-3 cells were maintained in Eagle's MEM supplemented with 10% endotoxin-free FBS, 5 μg/ml insulin, 0.2% glucose, and 0.2 ng/ml GM-CSF. For confocal imaging, Ca^{2+} measurements, phagocytosis assays, and ultrastructural studies, cells were seeded on 35-mm glass-bottom dishes (MatTek, Ashland, MA) without GM-CSF, and used after 48 h.

Construction of plasmids

The PKC-GFP (α, βI, βII, γ, δ, ε, η, and ζ) and GFP-DGK (α and γ) constructs were previously described (3, 18). Myristoylated alanine-rich C kinase substrate (MARCKS)-GFP and mutant MARCKS-GFP, whose all three putative PKC phosphorylation sites in the effector domain were substituted to Ala, were prepared as reported (19). DGKβ with the *Eco*RI site was produced by PCR, and was cloned into the *Eco*RI site in pEGFP-C1 (Clontech, Palo Alto, CA), and named as GFP-DGKβ. The C1 domain of δPKC (aa 159–280) with *Eco*RI/*Bgl*II sites was amplified by PCR, and was cloned into the *Eco*RI/*Bgl*II sites of BS 354 (19), and named as δPKC(C1)-GFP. The constructs encoding human $p47^{phox}$, $p67^{phox}$, and $p47^{phox}$(W193R) were previously described (20, 21). $p47^{phox}$ and $p47^{phox}$(W193R) was cloned into the *Bgl*II/*Eco*RI sites of pEGFP-C1, and named as GFP-$p47^{phox}$ and $p47^{phox}$(W193R), respectively.

Phagocytosis targets

IgG-opsonized glass beads (BIgG), fluorescently labeled BIgG, and control beads (BBSA) were prepared as described (3). Carboxylated latex beads were opsonized with IgG using the Carbodiimide kit (Polysciences).

Phagocytosis assay

The culture medium was replaced with $HBSS^{++}$ (3) and targets (50 per cell) were added. After incubation at 37°C for 20 min, cells were fixed with 4% PFA in 0.1 M phosphate buffer (pH 7.4). In inhibitor experiments, cells were preincubated in $HBSS^{++}$ containing the inhibitor. The number of completely engulfed targets per cell was counted in 50 cells using phase-contrast microscopy. The measurements were made in triplicate on at least three separate experiments, and results are presented as means ± SD.

Synchronized phagocytosis and cell fractionation

Synchronized phagocytosis and cell fractionation were performed as described with modifications (3, 22). The 6-3 cells in 10-cm dishes were treated with ice cold $HBSS^{++}$ (with or without inhibitor) containing BIgG (50 per cell). After 10 min on ice for target binding, the cells were warmed to 37°C for synchronized phagocytosis. At the indicated times, the cells were scraped and sonicated (3 × 10 s) in 400 μl of lysis buffer (18). The beads were allowed to settle 10 min on ice, and then the settled beads were sonicated again (2 × 10 s) to gain the phagosomal membrane. The beads were settled for 1 h, and the supernatant was centrifuged for 30 min at 100,000 × *g*. The pellet was solubilized in lysis buffer containing 1% Triton X-100. The samples were centrifuged again as above. The supernatant was designated as the membrane fraction containing the phagosomal membrane. After protein assay with bicinchoninic acid (Pierce, Rockford, IL), equal amounts of the membrane fraction (micrograms per lane) were subjected to SDS-PAGE and Western blotting (18).

Confocal imaging

The 6-3 cells were transfected using Superfect (Qiagen, Valencia, CA). After 24–30 h, the culture medium was replaced with 800 μl of $HBSS^{++}$, and cells were imaged using an LSM 510 invert (Carl Zeiss, Jena, Germany) confocal laser scanning fluorescence microscope with a heated stage and objective (×40 oil). Two hundred microliters of $HBSS^{++}$-containing targets (5 per cell) was added to each plate. To treat cells with inhibitor, the culture medium was replaced by a $HBSS^{++}$-containing inhibitor and preincubated for the indicated time. The images were collected at 3, 5, or 10 s intervals for 10 min. The time of addition of BIgG was chosen as time 0. In a 1-day experiment, >3 independent cell preparations (dishes) in each group were performed. In one dish, 1–3 cells which engulfed 1–5 BIgG for 10 min were selected for analysis in the study.

Ca^{2+} measurement

The 6-3 cells were loaded with 5 μM Fura 2-AM in HEPES buffer (18). After a 1-h incubation, the cells were resuspended in HEPES buffer. Fluorescence was monitored using the ARGUS/HiSCA system (Hamamatsu Photonics, Hamamatsu, Japan) using a dual wavelength excitation (340 and 380 nm) and at emission (510 nm). HEPES buffer containing targets (1 per cell) was added, and the images were collected at 1.5 s intervals for 5 min. In inhibitor experiments, cells were further incubated for the indicated time with HEPES buffer containing Fura 2-AM and the inhibitor. Cells were maintained at 37°C with a heated objective (×40 oil). Data are presented as the background-corrected 340:380 ratio of Fura 2 fluorescence.

O_2^- production assay

O_2^- production was determined as superoxide dismutase-inhibitable chemiluminescence (Diogenes; National Diagnostics, Atlanta, GA) as described previously (21). After the addition of the luminol-based substrate, the prewarmed cells (1.0×10^4) in $HBSS^{++}$ were stimulated with BIgG (1.0×10^5). The chemiluminescence was assayed for 20 min using a luminometer (Auto Lumat LB953; EG & G Berthold, Bad Wildbad, Germany).

In inhibitor experiments, cells were preincubated in an $HBSS^{++}$-containing inhibitor. The 6-3 cells incubated with stimulus in the absence of the inhibitor served as the positive control. Results are presented as the percent of the positive control (means ± SD).

Ultrastructural detection of an oxidant-producing site

The O_2^--producing site in 6-3 cells was detected using the cerium-based cytochemical method (23) with modifications (24). The reaction for the detection of H_2O_2 proceeds as follows: $NADPH + 2O_2 \rightarrow NADP^+ + H^+ + 2O_2^-$, $2O_2^- + 2H^+ \rightarrow H_2O_2 + O_2$, $H_2O_2 + CeCl_3 \rightarrow Ce(OH)_2OOH$, $Ce(OH)_3OOH$. The final cerous reaction products can be detected in the electron microscope as a precipitate. Treatment with the O_2^- scavenger, *p*-benzoquinone, causes complete abolishment of the reaction precipitate (24). The cells stimulated with either BIgG (latex, 5 per cells) or 1 μM PMA were incubated for 15 min at 37°C in HEPES buffer containing 1 mM $CeCl_3$, 1 mM NaN_3, and 20 mM tricine. NaN_3 was added to prevent the degradation of H_2O_2 by endogenous catalase. Tricine was used to protect Ce^{3+} in the reaction buffer from nonenzymatic precipitation. Exogenous NADPH and FAD are not necessary for the oxidant production in this method. The cells were fixed with 2% glutaraldehyde in HEPES buffer. After a cytochemical reaction, the cells were postfixed and then dehydrated and embedded in epoxy resin. Semithin sections (0.5 μm in thickness) were observed under a JEM-100S electron microscope (JEOL, Tokyo, Japan).

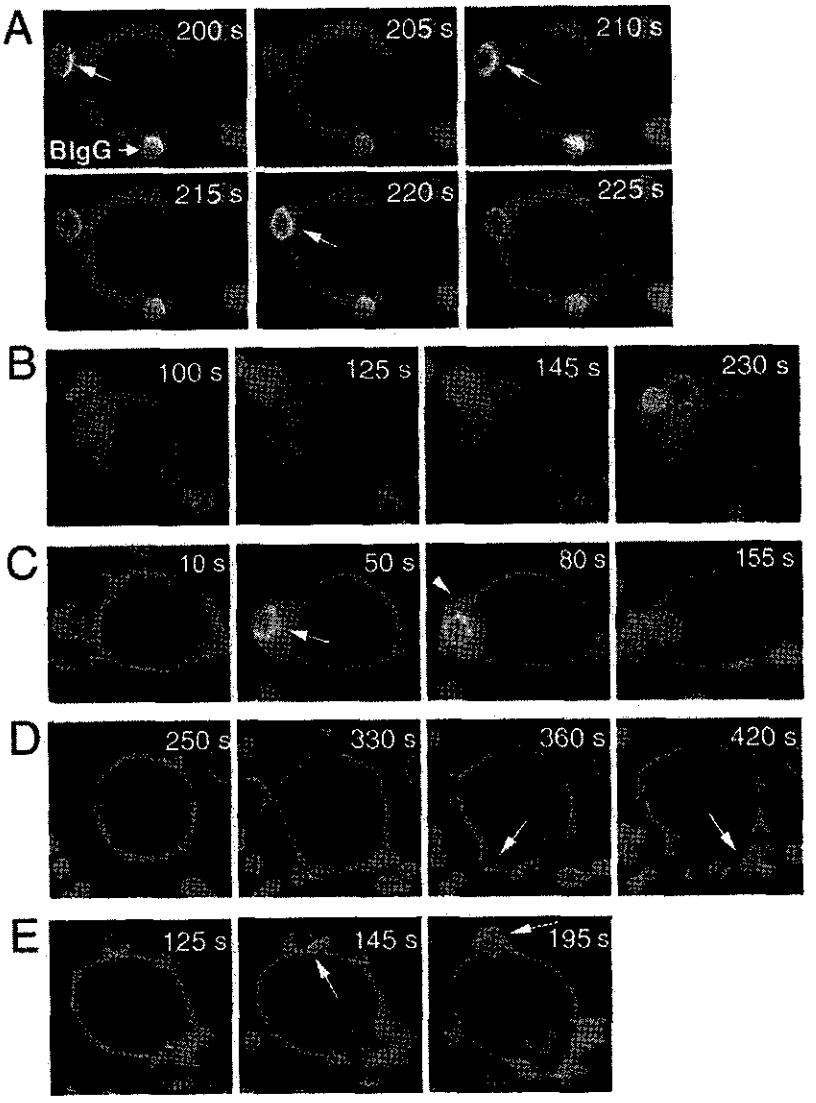

FIGURE 1. Accumulation of βI and εPKC, and DGKβ during FcγR-mediated phagocytosis. *A*, Oscillations in the accumulation of βI PKC-GFP at the phagosomal cup/phagosome is shown (arrows; cycle of oscillation is ~10 s; $n = >20$). No translocation of βI PKC-GFP to the plasma membrane is observed. A movie is available in Video 1. *B*, εPKC-GFP accumulates at the phagosomal cup/phagosome without oscillation ($n = >15$). *C*, GFP-DGKβ accumulates at the phagosomal cup (arrows) and at the plasma membrane (arrowhead), where BIgG was ingested. The accumulation was not apparent at the phagosome ($n = >20$). A movie is available in Video 2. *D*, MARCKS-GFP is released from the membrane of forming phagosome during internalization of BIgG (arrows; $n = >9$). *E*, The mutant MARCKS-GFP accumulated and was retained at the phagosomal cup and the forming phagosomal membrane (arrow) during internalization of BIgG.

Supporting information

The supplemental movies show the oscillatory accumulation of βI PKC-GFP (Video 1[4]) and the accumulation of DGKβ-GFP (Video 2) during phagocytosis of fluorescently labeled BIgG. Video 3 shows the oscillatory increase of $[Ca^{2+}]_i$ during phagocytosis of BIgG. Each movie represents >15 independent experiments.

Results

Characteristics of 6-3 microglial cells as phagocytes

We identified the PKC and type I DGK isoforms expressed in 6-3 microglial cells. Proteins of α, βI, δ, ε, η, and ζPKC and mRNAs for DGK α, β, and γ were detected by Western blotting and RT-PCR, respectively (data not shown); βII and γPKC were not detected in 6-3 cells. Expression of gp91^{phox}, p22^{phox}, p47^{phox}, p67^{phox}, and p40^{phox} in 6-3 cells was confirmed by Western blotting; and expression of Rac1 and Rac2, but not Rac3, were confirmed by RT-PCR (data not shown). PMA-stimulated O_2^- production in 6-3 cells was about one-tenth of that observed in neutrophils (data not shown).

[4] The on-line version of this article contains supplemental material.

Isoform-specific accumulation of PKC-GFP and GFP-DGK in Fcγ-mediated phagocytosis

Of the six PKC isoforms (α, βI, δ, ε, η, and ζ PKC) expressed, only βI and εPKC-GFP showed the localized translocation to the phagosomal cup/phagosome during phagocytosis of BIgG in 6-3 cells (Fig. 1, *A* and *B*, and Video 1). GFP-DGKβ was mainly localized on the plasma membrane before stimulation. Among type I DGK, only GFP-DGKβ accumulated without oscillation at the phagosomal cup, but not at the closed phagosome, during ingestion of BIgG. Accumulation of GFP-DGKβ briefly persisted at the plasma membrane where BIgG was ingested after closure of the phagosome (Fig. 1*C* and Video 2). More than 85% of the cells showed the accumulation of βI PKC-GFP, εPKC-GFP, and GFP-DGKβ (βI PKC-GFP < εPKC-GFP). Control beads (BBSA) were rarely phagocytosed by 6-3 cells (BBSA, 0.5 ± 0.1 per cell; BIgG, 8.4 ± 1.3 per cell), and did not cause any accumulation of above-mentioned molecules.

Different accumulation of βI and εPKC-GFP in FcγR-mediated phagocytosis

The time courses and patterns of the accumulation of βI PKC-GFP and εPKC-GFP were quite different. Localization times

were calculated and defined as T_1, time from the first concentration of PKC-GFP at the phagosomal cup until closure of the phagosome; T_2, time from closure of the phagosome until the signal returned to cytosolic levels; and T_t, $T_1 + T_2$. A repetitive accumulation of βI PKC-GFP was observed at the phagosomal cup and subsequently at the phagosome (19 of 22 cells; Fig. 1*A* and Video 1). The oscillatory accumulation of βI PKC-GFP occurred from 1 to 4 times (1, $n = 2$; 2, $n = 6$; 3, $n = 7$; and 4, $n = 4$) and was divided into two patterns; 1) accumulation only at the phagosomal cup, and 2) accumulation at both the cup and the phagosome. In accumulation pattern 2, T_1, T_2, and T_t were 24 ± 5, 21 ± 4, and 46 ± 7 s, respectively ($n = 10$). In contrast, εPKC-GFP accumulated at the phagosomal cup/phagosome without oscillation, and persisted longer (T_1, 26 ± 6 s; T_2, 93 ± 19 s; T_t, 119 ± 19 s; $n = 10$; Fig. 1*B*).

We used MARCKS-GFP as an indicator of the active PKC. MARCKS-GFP is constitutively present on the plasma membrane in an unphosphorylated form and is released from the membrane upon phosphorylation by PKC (19). In the present study, the loss of membrane-associated MARCKS-GFP was observed only at regions of the plasma membrane containing BIgG (Fig. 1*D*). Although not definitive, this evidence is consistent with the presence of active PKC in the forming phagosome. This conclusion is strengthened by the use of a mutant MARCKS-GFP that cannot be phosphorylated by PKC (19). This mutant MARCKS-GFP accumulated and was retained at the phagosomal cup and the forming phagosomal membrane during internalization of BIgG (Fig. 1*E*).

To validate that the GFP constructs mimic their endogenous counterparts, we measured the translocation of endogenous βI and εPKC during FcγR-mediated phagocytosis in 6-3 cells. βI and εPKC increased in the membrane fraction of nontransfected 6-3 cells in a time-dependent fashion (Fig. 2). Similar to the results with GFP conjugates, the increase in membrane-associated εPKC was sustained longer than that of βI PKC (Fig. 2).

Mechanism of oscillatory accumulation of βI PKC-GFP in FcγR-mediated phagocytosis

We have reported that εPKC, but not cPKC, enhances the rate of BIgG uptake, and that inhibition of εPKC causes ~50% inhibition of FcγR-mediated phagocytosis (3). Therefore, we focused on clarifying the accumulation/activation mechanism and the functional role of βI PKC in the present study. The accumulation of βI PKC-GFP was abolished by 2 μM U73122, an inhibitor of PLC (9), but not its inactive analog, U73343 (Fig. 3*A*). Pretreatment with R59949, an inhibitor of type I DGK, enhanced the accumulation of βI PKC-GFP, and induced the translocation of βI PKC-GFP to the plasma membrane (Fig. 3*B*). This result was confirmed by fractionation experiments. Treatment with R59949 increased the amount of membrane-associated βI PKC (Fig. 3, *C* and *D*).

To clarify the mechanism of βI PKC-GFP oscillations, $[Ca^{2+}]_i$ increase, and the production of DAG during phagocytosis were examined. One phagocytic event resulted in 1–4 $[Ca^{2+}]_i$ oscillations as determined by an increase in the 340:380 ratio of Fura 2 fluorescence (Fig. 4*A* and Video 3). Pretreatment with 2 μM U73122, but not U73343, significantly suppressed the amplitude of $[Ca^{2+}]_i$ increase (Fig. 4*B*). δPKC(C1)-GFP, a DAG indicator (9), transiently accumulated at the phagosomal cup/phagosome without oscillation (Fig. 4*C*). U73122 inhibited the accumulation of δPKC(C1)-GFP in dose-dependent manner (data not shown). Both Ca^{2+} and DAG are necessary for the full-activation of cPKC on the membrane (25). Taken together, these results are consistent with a model in which the oscillations of βI PKC-GFP during

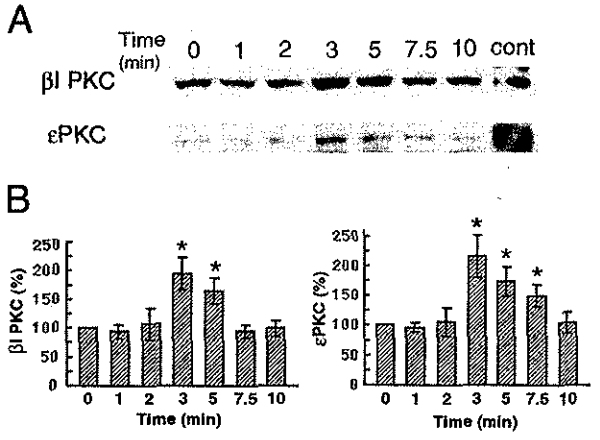

FIGURE 2. Translocation of endogenous βI and εPKC to the membrane fraction during synchronized phagocytosis of BIgG. *A*, βI PKC in the membrane fraction increases from 3 to 5 min. The increase of εPKC in the membrane fraction is sustained longer than that of βI PKC from 3 to 7.5 min. Representative of four experiments; cont, positive control from rat brain. *B*, Quantitation of membrane-associated βI PKC and εPKC during synchronized phagocytosis. Quantitative image analysis was performed using a NIH image. *, Significantly greater than 0 time point; $p < 0.05$.

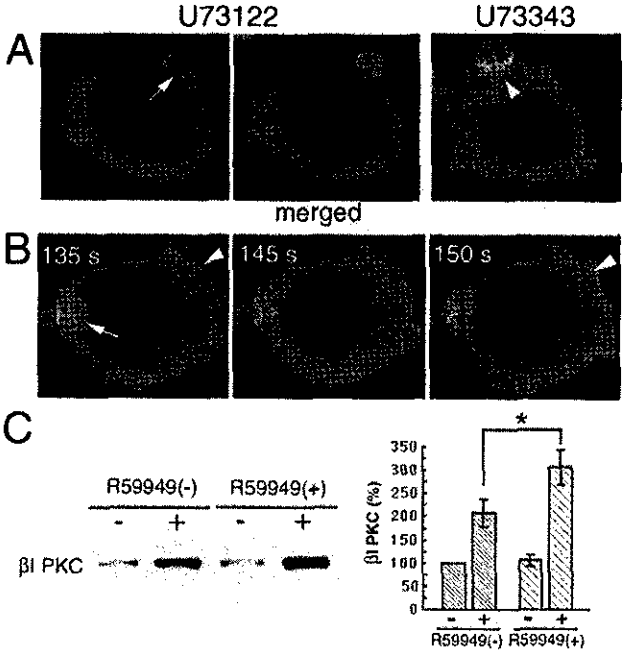

FIGURE 3. Mechanism of accumulation of βI PKC in FcγR-mediated phagocytosis. *A*, The accumulation of βI PKC-GFP is blocked by pretreatment with 2 μM U73122 for 15 min (arrow; $n = >9$). In contrast, βI PKC-GFP is recruited normally to the phagosomal cup in the presence of 2 μM U73343 for 15 min (arrowhead; $n = >9$). *B*, Pretreatment with 50 μM R59949 for 15 min enhances the accumulation of βI PKC-GFP (arrow; $n = >9$). It also induces the translocation of βI PKC-GFP to the plasma membrane (arrowheads). *C*, Translocation of endogenous βI PKC to the membrane fraction during synchronized phagocytosis of BIgG is enhanced by 10 μM R59949. With the DGK inhibitor (R59949(+)), the maximum increase of βI PKC in the membrane fraction (6 min) was greater than that without the inhibitor (R59949(−) 4 min). Representative of four experiments; −, without BIgG stimulation; +, with BIgG stimulation. *D*, Quantitation of maximum increase of membrane-associated βI PKC with or without R59949 during synchronized phagocytosis. Quantitative image analysis was performed using a NIH image. *, $p < 0.05$; −, without BIgG stimulation; +, with BIgG stimulation.

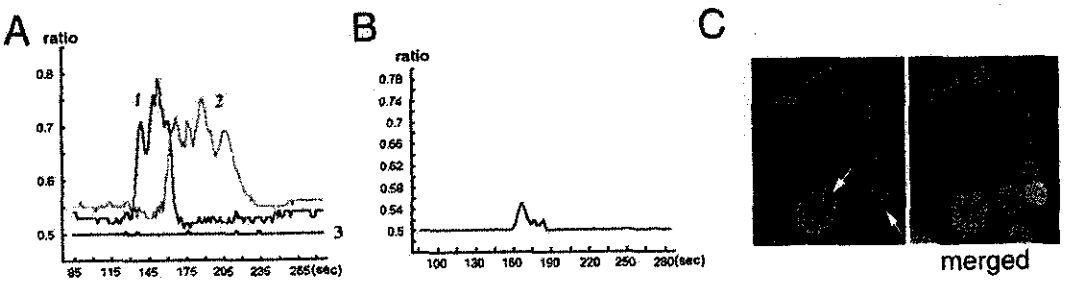

FIGURE 4. Mechanism of oscillatory accumulation of βI PKC in FcγR-mediated phagocytosis. *A*, Quantitation of $[Ca^{2+}]_i$ oscillations during phagocytosis (n = >20). The cells corresponding to each profile are identified in Video 3 (supporting information). Cell 1 (blue line) showing two $[Ca^{2+}]_i$ oscillations (duration, 39 s) and cell 2 (purple line) generating four oscillations (duration, 60 s) each ingested one BIgG (as determined by phase-contrast microscopy after the measurement). Cell 3 (black line) shows no $[Ca^{2+}]_i$ increase because there was no phagocytosis. *B*, Pretreatment with 2 μM U73122 for 15 min significantly suppresses the amplitude of $[Ca^{2+}]_i$ increase (n = >9). *C*, δPKC(C1)-GFP, a DAG indicator, accumulates at the phagosome (arrows; n = >20).

BIgG ingestion are due to parallel $[Ca^{2+}]_i$ oscillations in cooperation with localized DAG production at the phagosomal cup/phagosome.

O_2^- production during FcγR-mediated phagocytosis

We measured O_2^- production in 6-3 cells during FcγR-mediated phagocytosis using a superoxide dismutase-inhibitable luminal-based detection system (21).

O_2^- production was abolished by 100 nM Gö6976, a selective inhibitor of cPKC (1.64 ± 0.1% of uninhibited controls) or 2 μM U73122, a PLC inhibitor (0.1 ± 0.0%). In contrast, 10 μM R59949 increased O_2^- production 4.37-fold (Table I). O_2^- production was inhibited by Gö6976 (0–300 nM) and enhanced by R59949 (0–10 μM) in a dose-dependent manner (Fig. 5). As βI PKC is the only cPKC associated with phagosomes in 6-3 cells, and Gö6976 effectively blocks O_2^- production, this data supports a model in which βI PKC mediates O_2^- release. The fact that U73122 mimics the Gö6976 effect with respect to the inhibition of O_2^- release is consistent with the activation of βI PKC via PLC-derived DAG and IP_3-mediated rise in $[Ca^{2+}]_i$. However, Gö6976 did not affect the accumulation of βI PKC (Table I), providing evidence that βI PCK activity, rather than localization, is necessary for O_2^- production.

Oxidant-producing site during FcγR-mediated phagocytosis

PKC phosphorylates $p47^{phox}$, acting as the major activating kinase for the NADPH oxidase (11). We tested the hypothesis that accumulation of βI PKC corresponds with the temporal localization of $p47^{phox}$. In 6-3 cells expressing GFP-$p47^{phox}$ and $p67^{phox}$, GFP-$p47^{phox}$ accumulated at the phagosomal cup/phagosome without oscillation (T_t, 65 ± 7; n = 5; Fig. 6*A*), but not on nontarget-associated plasma membranes. GFP-$p47^{phox}$(R193W), which does not bind to $p22^{phox}$ nor produce O_2^- (20), did not accumulate at the phagosomal cup/phagosome (Fig. 6*B*). The accumulation of GFP-$p47^{phox}$ was not enhanced by pretreatment with R59949 (data not shown).

Because βI PKC-GFP and GFP-$p47^{phox}$ accumulated at the phagosomal cup/phagosome during phagocytosis of BIgG, we hypothesized that NADPH oxidase could be activated only at the site of PKC accumulation. We used electron microscopy to visualize the intracellular site of H_2O_2 production (dismutated from O_2^- generated by NADPH oxidase) in response to either BIgG or PMA. In 6-3 cells, the reaction product stimulated by BIgG was detected only at the phagosome (Fig. 7*A*), while that by PMA was at the intracellular granules (Fig. 7*B*). No reaction precipitate was found in cells incubated in the absence of $CeCl_3$, BIgG, or PMA (data not shown). These results show that oxidant production during FcγR-stimulated phagocytosis initiates at the phagosomal cup/phagosome, but not at the intracellular granules.

Discussion

This study and one recent report showed that NADPH oxidase functions in the microglia of the CNS (26). The present study is a first report of the visualizing the signal transduction pathway during FcγR-mediated respiratory burst at the cellular level in microglia. There are many reports that multiple PKC isoforms (α, β, δ, ε and ζPKC) involved in phagocytosis (22, 27). In 6-3 microglial cells, PKC isoforms α, βI, δ, ε, η, and ζPKC were expressed, and only βI and εPKC-GFP, but not α, δ, η, or ζPKC-GFP, accumulated at the phagosomal cup/phagosome, but not on the plasma membrane, during phagocytosis of BIgG. These findings are intriguing that receptor ligation not only controls which PKC isoform translocates but also the membranes to which they localize. There is a report that dominant negative αPKC impaired FcγR-mediated phagocytosis in RAW macrophages (28). However, we have reported that cPKC mediates the FcγR-stimulated respiratory burst, and that nPKC is necessary for phagocytosis in RAW cells (22). More recently, we have demonstrated that εPKC, but not cPKC, enhances the rate of BIgG uptake, and that inhibition of εPKC causes ~50% inhibition of FcγR-mediated phagocytosis (3). In microglia, no accumulation of αPKC-GFP was observed during BIgG ingestion, and a selective inhibitor of cPKC did not

Table I. *Effects of PKC, PLC, and DGK inhibitors on 6-3 cell function in FcγR-mediated phagocytosis*[a]

	Gö6976	U73122	U73343	R59949
O_2^- production	1.64 ± 0.1 %**	0.1 ± 0.0 %**	110.4 ± 2.2 %*	436.9 ± 16.1 %**
Phagocytosis	97.5 ± 9.0 %	65.9 ± 6.6 %**	98.0 ± 5.2 %	118.6 ± 9.3 %**
βI PKC accumulation	+	−	+	++

[a] Results are presented as a percentage of uninhibited controls (means ± SD %; $n \geq 4$). +, ++, and − means normal, enhanced, and abolished accumulation, respectively. Gö6976 was used at 500 nM (100 nM for measurement of O_2^-) for −15 min prior to the addition of stimulus. Pretreatment with 2 μM U73122 and U73343 was done for 15 min: R59949 was used at 10 μM for 15 min. O_2^- production was determined using a luminol-based detection system. See text for details. **, $p < 0.01$ and *, $p < 0.05$.

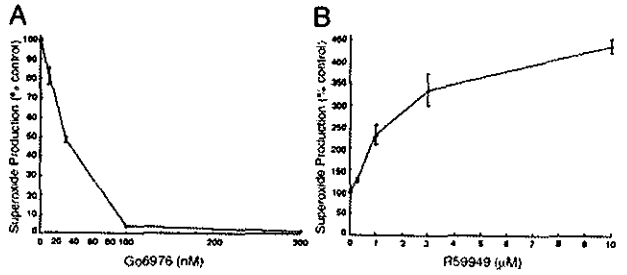

FIGURE 5. Dose-dependent inhibition of O_2^- production by Gö6976 (*A*) or enhancement by R59949 (*B*) in FcγR-mediated phagocytosis. Data are obtained from at least four independent experiments and expressed as means ± SD.

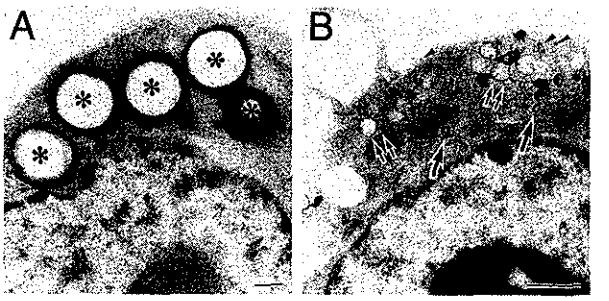

FIGURE 7. Representative electron micrographs of the oxidant production site in response to BIgG (latex; *A*; $n = 15$), and PMA (*B*; $n = 9$). The former reveals the reaction product only around BIgG in the phagosome (asterisks). The latter shows the reaction product at intracellular compartments consisting of vesicles (arrows), vacuoles (double arrows), and smaller vesicles (arrowheads) near the plasma membrane. Bars, 1 μm.

change the phagocytosis (Table I). Taken together, FcγR efficiently couples to βI PKC to facilitate O_2^- production in microglia. In addition, accumulation of εPKC had a good correlation with BIgG uptake in microglia as macrophages (our unpublished data). In the present study, we also showed the apparent differences of the accumulation patterns between βI PKC-GFP and εPKC-GFP. Two signals, one the locally produced DAG at the phagosomal cup/phagosome by PLCγ and the other the $[Ca^{2+}]_i$ oscillations by PLCγ, acting in concert are required for activation of βI PKC during FcγR-mediated phagocytosis. In an earlier study, stepwise phosphorylation of $p47^{phox}$ by PMA was indeed reported: although the final phosphorylation event of $p47^{phox}$ initiating O_2^- production occurs at membrane components, the first phosphorylation of $p47^{phox}$ promoting its translocation to membrane components primarily occurs in cytosol (29). We showed that accumulation of $p47^{phox}$ was not oscillatory, supporting a model that phosphorylated $p47^{phox}$ tightly associates with membrane (29). Recently, Dewitt et al. (30) reported that the first $[Ca^{2+}]_i$ increase is not sufficient for O_2^- production. The possibility exists that the oscillatory signal by βI PKC between the phagosomal cup/phagosome and cytosol are used for both initialization of membrane translocation of $p47^{phox}$ in cytosol and tight association of $p47^{phox}$ to membrane and full activation of the NADPH oxidase at membrane. However, the physiological contributions of the oscillatory accumulation of βI PKC is presently unclear.

In vitro, $p47^{phox}$ is phosphorylated on 8–10 serine residues within its C-terminal region by different types of protein kinases; one or more PKC family members are indicated to play a major role (31). Phosphopeptide mapping of $p47^{phox}$ showed that α, β, and δPKC phosphorylated all major peptides, although δPKC was less active toward some peptides; phosphorylation by ζPKC was only a few peptides (11). Using neutrophils from βPKC null mice, Dekker et al. (5) reported that the lack of βPKC decreased the amount of O_2^- production by 50% stimulated by BIgG and PMA, and they also demonstrated a significant inhibition of O_2^- production stimulated by PMA and IgG-opsonized bacteria in human neutrophils treated with a βPKC-specific inhibitor (5). It was also reported that a similar degree of inhibition of O_2^- production by PMA, immune complex, and fMLP in human HL60 cells using an antisense method *(32)*. In contrast, αPKC, but not βPKC, is involved in O_2^- production by BIgG (22) and by opsonized zymosan (33), in monocytes. Although apparently disparate, these results suggest that βPKC contributes to the respiratory burst in neutrophils while αPKC performs this function in monocytes. The present study is consistent with microglia using a neutrophil-like pathway for PKC regulation of O_2^- production. Furthermore, recent reports show that βPKC and δPKC bind to $p47^{phox}$ in intact neutrophils stimulated by PMA with different time courses (34), and ζPKC participates in the fMLP-induced, but not PMA-induced, respiratory burst (35). It was also reported that ζPKC accumulated on the phagosome during ingestion of *Helicobacter pylori*, but not IgG-opsonized *H. pylori* (36), in monocytes. Thus, it is likely that different receptors are coupled to the specialized signaling networks and use different PKC isoforms. Taken together,

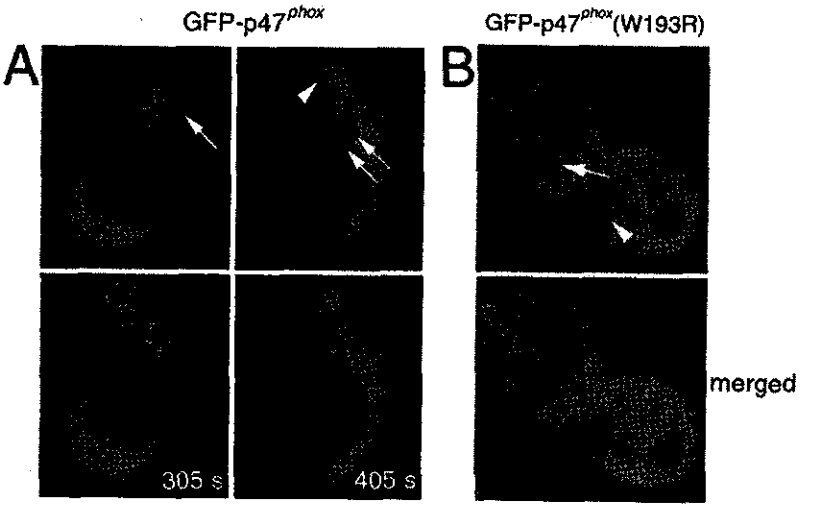

FIGURE 6. Accumulation of $p47^{phox}$ during FcγR-mediated phagocytosis. *A*, At 305 s, GFP-$p47^{phox}$ accumulation is apparent at the phagosome (arrow). By 405 s, the accumulation has disappeared (double arrows); weak accumulation of GFP-$p47^{phox}$ at a forming phagosomal cup is indicated by the arrowhead. Translocation of GFP-$p47^{phox}$ to the plasma membrane is not observed ($n = >12$). *B*, GFP-$p47^{phox}$(R193W) does not accumulate at any time point (arrow, phagosome; arrowhead, phagosomal cup; $n = >12$).

use of PKC isoform likely is determined by both the cell type and the stimulus.

O_2^- can be produced either extracellularly or within the phagosome during phagocytosis. Extracellular O_2^- is thought to originate from either the phagosomal cup or the plasma membrane. In the present study, during the ingestion of BIgG, βI PKC-GFP and GFP-p47^{phox} translocated to the phagosomal cup/phagosome, but not to the plasma membrane. These results indicate that the extracellular O_2^- primarily originates from the phagosomal cup. DAG is one of the key lipid mediators in O_2^- production (37, 38). Inhibition of DGK with R59949 significantly enhanced O_2^- production and induced the translocation of βI PKC-GFP to the plasma membrane in addition to the enhanced accumulation at the phagosomal cup/phagosome. However, the accumulation of GFP-p47^{phox} was not enhanced by pretreatment with R59949, this result suggests that DAG may not be primarily associated with the translocation of p47^{phox} and enhanced O_2^- production may be primarily from the enhanced accumulation of βI PKC at the phagosomal cup/phagosome. Furthermore, DGKβ accumulated on the forming phagosome, but not at the closed phagosome, while βI PKC and p47^{phox} accumulated both at the phagosomal cup and phagosome. Thus, DGKβ which is localized on the plasma membrane in resting states, accumulates on the forming phagosome, and briefly stays at the phagocytosis-involved plasma membrane after closure of the phagosome, likely plays an important role in control of excessive secretion of O_2^- to the extracellular milieu through regulation of βI PKC activation during phagocytosis rather than termination of O_2^- production. This is consistent with a report that termination of O_2^- production correlated with dissociation of p47^{phox}/p67^{phox} complex from the phagosome (39). Because βI PKC accumulated at the phagosomal cup from initiation of phagocytosis and inhibition of βI PKC showed a profound decrease of O_2^- production, βI PKC most likely plays a key role for initiation of respiratory burst, at least. Other pathways, such as PI3K pathway, likely contribute to the later stage of O_2^- production (40). In agreement with this idea, GFP-tagged PX domain of p40^{phox}, a phosphatidylinositol 3-phosphate indicator, accumulated at the phagosome only after closure of the phagosome (our unpublished data).

It has been reported that cytochrome b_{558} is primarily localized on intracellular granules (~80%) in neutrophils (41). Recently, it was reported that O_2^- production stimulated by PMA initially takes place at intracellular granules, followed by fusion of these granules with the plasma membrane, resulting in the delivery of O_2^- into the extracellular milieu (13, 14). However, because βI PKC-GFP and GFP-p47^{phox} accumulated at the phagosomal cup/phagosome in this study, we hypothesized that NADPH oxidase could be activated primarily at the phagosomal cup/phagosome during FcγR-mediated phagocytosis in microglia. Our present results using electron microscopy supported that oxidant production during FcγR-stimulated phagocytosis initiates at the phagosomal cup/phagosome where DAG is locally formed during BIgG ingestion, but not at the intracellular granules. In contrast, consistent with previous reports, PMA caused the oxidant production at the intracellular granules. We propose that O_2^- production during FcγR-stimulated phagocytosis begins at the phagosomal cup/phagosome through phosphorylation of p47^{phox} by cPKC. Although microglia use βPKC as neutrophils do, and macrophages use αPKC, the basis of this model may be adapted to all phagocytes in FcγR-stimulated phagocytosis. In support of our results, it was reported that, based on stoichiometry, O_2^- is formed at the phagosomal cup/phagosome during phagocytosis of opsonized zymosan in neutrophils (42). When phagocytosis is blocked by cytochalasin B, O_2^- is formed at the phagosomal cup (cell-zymosan interface) only and secreted into the extracellular milieu (S. Kanegasaki, Tokyo University, unpublished observation). Microglia had only about one-tenth capacity for O_2^- production compared with neutrophils. Further elucidation, especially about the assembly of NADPH oxidase complex during FcγR-stimulated phagocytosis at the cellular level, is required.

Acknowledgments

We thank Dr. Kaoru Goto (Yamagata University School of Medicine, Yamagata, Japan) for providing the cDNA for rat DGKβ.

References

1. Greenberg, S., and S. Grinstein. 2002. Phagocytosis and innate immunity. *Curr. Opin. Immunol. 14:136.*
2. Bard, F., C. Cannon, R. Barbour, R. L. Burke, D. Games, H. Grajeda, T. Guido, K. Hu, J. Huang, K. Johnson-Wood, et al. 2000. Peripherally administered antibodies against amyloid β-peptide enter the central nervous system and reduce pathology in a mouse model of Alzheimer disease. *Nat. Med. 6:916.*
3. Larsen, E. C., T. Ueyama, P. M. Brannock, Y. Shirai, S. Saito, C. Larsson, D. J. Loegering, P. B. Weber, and M. R. Lennartz. 2002. A role for PKC-ε in FcγR-mediated phagocytosis by RAW 264.7 cells. *J. Cell Biol. 159:939.*
4. Leitges, M., C. Schmedt, R. Guinamard, J. Davoust, S. Schaal, S. Stabel, and A. Tarakhovsky. 1996. Immunodeficiency in protein kinase Cβ-deficient mice. *Science 273:788.*
5. Dekker, L. V., M. Leitges, G. Altschuler, N. Mistry, A. McDermott, J. Roes, and A. W. Segal. 2000. PKC-β contributes to NADPH oxidase activation in neutrophils. *Biochem. J. 347(Pt. 1):285.*
6. Castrillo, A., D. J. Pennington, F. Otto, P. J. Parker, M. J. Owen, and L. Bosca. 2001. *PKCε is required* for macrophage activation and defense against bacterial infection. *J. Exp. Med. 194:1231.*
7. Kanoh, H., K. Yamada, and F. Sakane. 2002. Diacylglycerol kinases. *J. Biochem. 131:629.*
8. Bokoch, G. M., and U. G. Knaus. 2003. NADPH oxidases: not just for leukocytes anymore! *Trends Biochem. Sci. 28:502.*
9. Botelho, R. J., M. Teruel, R. Dierckman, R. Anderson, A. Wells, J. D. York, T. Meyer, and S. Grinstein. 2000. Localized biphasic changes in phosphatidylinositol-4,5-bisphosphate at sites of phagocytosis. *J. Cell Biol. 151:1353.*
10. Babior, B. M. 1999. NADPH oxidase: an update. *Blood 93:1464.*
11. Fontayne, A., P. M. Dang, M. A. Gougerot-Pocidalo, and J. El-Benna. 2002. Phosphorylation of p47^{phox} sites by PKC α, βII, δ, and ζ. *Biochemistry 41:7743.*
12. Hoyal, C. R., A. Gutierrez, B. M. Young, S. D. Catz, J. H. Lin, P. N. Tsichlis, and B. M. Babior. 2003. Modulation of p47^{phox} activity by site-specific phosphorylation: Akt-dependent activation of the NADPH oxidase. *Proc. Natl. Acad. Sci. USA 100:5130.*
13. Kobayashi, T., J. M. Robinson, and H. Seguchi. 1998. Identification of intracellular sites of superoxide production in stimulated neutrophils. *J. Cell Sci. 111:81.*
14. Brown, G. E., M. Q. Stewart, H. Liu, V. L. Ha, and M. B. Yaffe. 2003. A novel assay system implicates PtdIns(3,4)P(2), PtdIns(3)P, and PKCδ in intracellular production of reactive oxygen species by the NADPH oxidase. *Mol. Cell. 11:35.*
15. Sawada, M., F. Imai, H. Suzuki, M. Hayakawa, T. Kanno, and T. Nagatsu. 1998. Brain-specific gene expression by immortalized microglial cell-mediated gene transfer in the mammalian brain. *FEBS Lett. 433:37.*
16. Kanzawa, T., M. Sawada, K. Kato, K. Yamamoto, H. Mori, and R. Tanaka. 2000. Differentiated regulation of allo-antigen presentation by different types of murine microglial cell lines. *J. Neurosci. Res. 62:383.*
17. Inoue, H., M. Sawada, A. Ryo, H. Tanahashi, T. Wakatsuki, A. Hada, N. Kondoh, K. Nakagaki, K. Takahashi, A. Suzumura, et al. 1999. Serial analysis of gene expression in a microglial cell line. *Glia 28:265.*
18. Shirai, Y., S. Segawa, M. Kuriyama, K. Goto, N. Sakai, and N. Saito. 2000. Subtype-specific translocation of diacylglycerol kinase α and γ and its correlation with PKC. *J. Biol. Chem. 275:24760.*
19. Ohmori, S., N. Sakai, Y. Shirai, H. Yamamoto, E. Miyamoto, N. Shimizu, and N. Saito. 2000. Importance of PKC targeting for the phosphorylation of its substrate, MARCKS. *J. Biol. Chem. 275:26449.*
20. Sumimoto, H., K. Hata, K. Mizuki, T. Ito, Y. Kage, Y. Sakaki, Y. Fukumaki, M. Nakamura, and K. Takeshige. 1996. Assembly and activation of the phagocyte NADPH oxidase. *J. Biol. Chem. 271:22152.*
21. Kuribayashi, F., H. Nunoi, K. Wakamatsu, S. Tsunawaki, K. Sato, T. Ito, and H. Sumimoto. 2002. The adaptor protein p40^{phox} as a positive regulator of the superoxide-producing phagocyte oxidase. *EMBO J. 21:6312.*
22. Larsen, E. C., J. A. DiGennaro, N. Saito, S. Mehta, D. J. Loegering, J. E. Mazurkiewicz, and M. R. Lennartz. 2000. Differential requirement for classic and novel PKC isoforms in respiratory burst and phagocytosis in RAW 264.7 cells. *J. Immunol. 165:2809.*
23. Briggs, R. T., D. B. Drath, M. L. Karnovsky, and M. J. Karnovsky. 1975. Localization of NADH oxidase on the surface of human polymorphonuclear leukocytes by a new cytochemical method. *J. Cell Biol. 67:566.*
24. Kobayashi, T., E. Garcia del Saz, J. Hendry, and H. Seguchi. 1999. Detection of oxidant producing-sites in glutaraldehyde-fixed human neutrophils and eosinophils stimulated with PMA. *Histochem. J. 31:181.*
25. Oancea, E., and T. Meyer. 1998. PKC as a molecular machine for decoding calcium and diacylglycerol signals. *Cell 95:307.*

26. Lavigne, M. C., H. L. Malech, S. M. Holland, and T. L. Leto. 2001. Genetic requirement of $p47^{phox}$ for superoxide production by murine microglia. *FASEB J. 15:285.*
27. Sergeant, S., and L. C. McPhail. 1997. Opsonized zymosan stimulates the redistribution of protein kinase C isoforms in human neutrophils. *J. Immunol. 159:2877.*
28. Breton, A., and A. Descoteaux. 2000. Protein kinase C-α participates in FcγR-mediated phagocytosis in macrophages. *Biochem. Biophys. Res. Commun. 276:472.*
29. Rotrosen, D., and T. L. Leto. 1990. Phosphorylation of neutrophil 47-kDa cytosolic oxidase factor: translocation to membrane is associated with distinct phosphorylation events. *J. Biol. Chem. 265:19910.*
30. Dewitt, S., I. Laffafian, and M. B. Hallett. 2003. Phagosomal oxidative activity during β_2 integrin (CR3)-mediated phagocytosis by neutrophils is triggered by a non-restricted Ca^{2+} signal: Ca^{2+} controls time not space. *J. Cell Sci. 116:2857.*
31. El Benna, J., R. P. Faust, J. L. Johnson, and B. M. Babior. 1996. Phosphorylation of the respiratory burst oxidase subunit $p47^{phox}$ as determined by two-dimensional phosphopeptide mapping: phosphorylation by protein kinase C, protein kinase A, and a mitogen-activated protein kinase. *J. Biol. Chem. 271:6374.*
32. Korchak, H. M., M. W. Rossi, and L. E. Kilpatrick. 1998. Selective role for β-protein kinase C in signaling for O_2^- generation but not degranulation or adherence in differentiated HL60 cells. *J. Biol. Chem. 273:27292.*
33. Li, Q., V. Subbulakshmi, A. P. Fields, N. R. Murray, and M. K. Cathcart. 1999. PKC α regulates human monocyte O_2^- production and low density lipoprotein lipid oxidation. *J. Biol. Chem. 274:3764.*
34. Reeves, E. P., L. V. Dekker, L. V. Forbes, F. B. Wientjes, A. Grogan, D. J. Pappin, and A. W. Segal. 1999. Direct interaction between $p47^{phox}$ and PKC. *Biochem. J. 344(Pt. 3):859.*
35. Dang, P. M., A. Fontayne, J. Hakim, J. El Benna, and A. Perianin. 2001. Protein kinase C ζ phosphorylates a subset of selective sites of the NADPH oxidase component $p47^{phox}$ and participates in formyl peptide-mediated neutrophil respiratory burst. *J. Immunol. 166:1206.*
36. Allen, L. A., and J. A. Allgood. 2002. Atypical PKC-ζ is essential for delayed phagocytosis of *Helicobacter pylori*. *Curr. Biol. 12:1762.*
37. Arnhold, J., S. Benard, U. Kilian, S. Reichl, J. Schiller, and K. Arnold. 1999. Modulation of luminol chemiluminescence of fMLP-stimulated neutrophils by affecting dephosphorylation and the metabolism of phosphatidic acid. *Luminescence 14:129.*
38. Erickson, R. W., P. Langel-Peveri, A. E. Traynor-Kaplan, P. G. Heyworth, and J. T. Curnutte. 1999. Activation of human neutrophil NADPH oxidase by phosphatidic acid or diacylglycerol in a cell-free system. *J. Biol. Chem. 274:22243.*
39. DeLeo, F. R., L. A. Allen, M. Apicella, and W. M. Nauseef. 1999. NADPH oxidase activation and assembly during phagocytosis. *J. Immunol. 163:6732.*
40. Karlsson, A., J. B. Nixon, and L. C. McPhail. 2000. PMA induces neutrophil NADPH-oxidase activity by two separate signal transduction pathways. *J. Leukocyte Biol. 67:396.*
41. Jesaitis, A. J., E. S. Buescher, D. Harrison, M. T. Quinn, C. A. Parkos, S. Livesey, and J. Linner. 1990. Ultrastructural localization of cytochrome *b* in the membranes of resting and phagocytosing human granulocytes. *J. Clin. Invest. 85:821.*
42. Makino, R., T. Tanaka, T. Iizuka, Y. Ishimura, and S. Kanegasaki. 1986. Stoichiometric conversion of oxygen to superoxide anion during the respiratory burst in neutrophils. *J. Biol. Chem. 261:11444.*

Available online at www.sciencedirect.com
SCIENCE DIRECT
Neuroscience Research 51 (2005) 73–80
Neuroscience Research
www.elsevier.com/locate/neures

Localization of cyclooxygenase-2 induced following traumatic spinal cord injury

Kayo Adachi[a], Yu Yimin[b], Kotaro Satake[b], Yukihiro Matsuyama[b], Naoki Ishiguro[b], Makoto Sawada[a], Yoko Hirata[c], Kazutoshi Kiuchi[c,*]

[a]*Joint Research Division for Therapies against Intractable Diseases, Institute for Comprehensive Medical Science, Fujita Health University, Toyoake, Aichi 470-1192, Japan*
[b]*Department of Orthopaedic Surgery, Nagoya University School of Medicine, Nagoya 466-8550, Japan*
[c]*Department of Biomolecular Science, Faculty of Engineering, Gifu University, 1-1 Yanagido, Gifu 501-1193, Japan*

Received 10 September 2003; accepted 4 October 2004

Abstract

Objective: Up-regulation of cyclooxygenase-2 (COX-2), a key enzyme in the synthesis of prostaglandins (PGs), is postulated to be involved in pathological processes of acute spinal cord injury (SCI). In the present study, we sought to clarify temporal and spatial expression patterns of the *COX-2* gene induced in the spinal cord after traumatic insults using a weight-drop technique.
Results: Reverse transcriptase-polymerase chain reaction (RT-PCR) revealed that COX-2 transcription in the spinal cord began to increase within 30 min, peaked at 3 h after injury. Western blotting analysis indicated that the deglycosylated COX-2 protein significantly increased 6 h after injury. Double-immunofluorescent staining analysis showed that COX-2 immunoreactivity was present only in endothelial cells of blood vessels, but not in neurons, astrocytes, monocytes, macrophages, or microglia 6 h after injury.
Conclusions: The results suggested that *COX-2* gene induction seems not to require any new protein synthesis and that its expression in endothelial cells may be a component of an inflammatory process after traumatic SCI.

Keywords: Cyclooxygenase-2; Endothelial cells; Pia matters; Blood vessels; Rat; Spinal cord injury; Weight-drop technique

1. Introduction

Cyclooxygenase (COX) is a rate-limiting enzyme that catalyzes steps in the prostaglandin biosynthesis of arachidonic acid to PGG_2 and then to PGH_2, which is an unstable and common precursor for all prostanoids; two distinct isoforms of COX have been cloned (Kujubu et al., 1991; DeWitt and Smith, 1998). COX-1 is constitutively expressed in most tissues (DeWitt, 1991), whereas COX-2 is undetectable in most mammalian tissues (Smith et al., 1996) but is induced in response to various cytokines (Kujubu and Herschman, 1992; O'Banion et al., 1992), growth factors (Sirois et al., 1993), and endotoxins (Feng et al., 1993). Recently, COX-2 induction in the central nervous system (CNS) by some stimuli, such as bacterial lipopolysaccharide (LPS) (Breder and Saper, 1996) and interleukin-1β (IL-1β) (Inoue et al., 1999; Serou et al., 1999) has been demonstrated, and it has been observed in various pathologic conditions, such as seizures (Yamagata et al., 1993), global ischemia-reperfusion (Nakayama et al., 1998), peripheral inflammation (Ichitani et al., 1997), and traumatic spinal cord injury (SCI)(Resnick et al., 1998; Tonai et al., 1999).

The pathological process in SCI is considered to consist of two steps: the primary mechanical injury and secondary damage induced by various biochemical reactions (Faden, 1993; Tator, 1995). In the secondary damage, numerous factors are thought to contribute at a molecular level to spinal cord impairment, and are derived from a reduction of microcirculation in tissue (Tator and Fehlings, 1991). We have previously reported the up-regulation of two genes; *iNOS* and *GDNF*, in the immediate early stage after SCI. NO

* Corresponding author. Tel.: +81 582932651; fax: +81 582301893.
E-mail address: kiuchi@biomol.gifu-u.ac.jp (K. Kiuchi).

0168-0102/$ – see front matter
doi:10.1016/j.neures.2004.10.007

produced by iNOS-positive macrophages seems to trigger apoptosis of any adjacent damaged cells during the early stage of traumatic SCI (Satake et al., 2000a), while GDNF induced in microglia and macrophage is considered to exert a protective effect on neurons following SCI (Satake et al., 2000b). Nuclear factor-κB (NF-κB) responsive elements are known to exist in the promoter region of the *COX-2* gene (Yamamoto et al., 1995; Jobin et al., 1998) as well as in *iNOS* (Chao et al., 1997; Nishiya et al., 2000; Madrigal et al., 2001) and *GDNF* genes (Tanaka et al., 2000). Recently it has been reported that COX-2 expression causes both pro- and anti-inflammatory process including the NF-κB-dependent transcription in epithelial cells (Poligone and Baldwin, 2001). Therefore, these three genes are considered to influence one another and the balance of their activities seems to determine neuronal survival or degeneration. However, the precise starting point of induction of the *COX-2* gene and the localization of COX-2 protein in the spinal cord following traumatic SCI still remain unclear. In the present study, using reverse transcriptase-polymerase chain reaction (RT-PCR), we determined the time course of *COX-2* gene induction and using double-immunofluorescent staining, we investigated whether COX-2 protein expression is up-regulated in neurons, astrocytes, macrophages, microglia or endothelial cells in rat spinal cord after traumatic SCI by a weight-drop technique.

2. Material and methods

2.1. Surgical procedure for traumatic SCI

Sprague–Dawley rats (8 weeks, male) were anesthetized with pentobarbital and laminectomies were performed at the T8–T10 level. Spinal cords were injured using the weight-drop technique according to Allen's method (Allen, 1914) with a slight modification. A plastic impounder (2-mm diameter) was placed gently on the exposed dura and a 10-g iron weight was dropped from a height of a 10 cm onto the impounder. The weight and impounder were immediately removed after impact and paravertebral muscle and skin were closed. Sham controls underwent the same operations but without spinal cord insult. Rats used in this study were treated strictly according to the NIH Guide for Care and Use of Laboratory Animals, and our protocol was approved by RIKEN.

2.2. RNA extraction and RT-PCR

Rats were again anesthetized with pentobarbital and their spinal cords from the top and bottom 1.5 cm of the lesion were removed at 30 min, 3 h, 6 h, 12 h, 1 day, 2 days, 3 days, and 1 weeks; similarly those of the sham controls (0 min and 3 h). They were immediately frozen with dry ice and stored at −80 °C until use. Total mRNA was prepared from cord segments using RNeasy Midi (Qiagen) and the resultant mRNA was reverse transcribed with oligo d(T) 12–18 using Superscript II (Invitrogen). This RT mixture was used as a template for PCR. PCRs were carried out in a GeneAmp PCR System 2400 (Applied Biosystems) using a protocol consisting of denaturation at 95 °C for 60 s, annealing at 60 °C for 60 s, and extension at 72 °C for 60 s in each of 35 cycles for COX-2 and 25 cycles for β-actin, respectively. The primer sets were COX-2; 5′-GAA CAA CAT TCC CTT CCT TCG-3′ and 5′-GAA GTT CCT TAT TTC CTT TCA CAC C-3′, and β-actin; 5′-TGT ATG CCT CTG GTC GTA CC-3′ and 5′-CAA CGT CAG ACT TCA TGA TGG-3′. The PCR products were electrophoresed through a 1.5% agarose gel containing ethidium bromide. Images were captured using a Gel Print 2000i/VGA (Bio Image), and the intensity ratio between the COX-2 and β-actin bands was determined using the computer software, Intelligent Quantifier (Bio Image).

2.3. Tissue preparation

Six hours after injury, rats were anesthetized with sodium pentobarbital (50 mg/kg) perfused through the ascending aorta with 4 ml of heparin (1000 U/ml in 0.9% NaCl) and with 20 ml of 4% (w/v) paraformaldehyde (PFA) in 0.1 M sodium phosphate buffer (PB), pH 7.4. Their spinal cords were removed and post-fixed for 4 h in 4% PFA at 4 °C. After cryoprotection in 30% sucrose for 3 days, they were embedded in OCT compound (Tissue TEK II, Miles), rapidly frozen in dry ice–acetone, and stored at −80 °C until

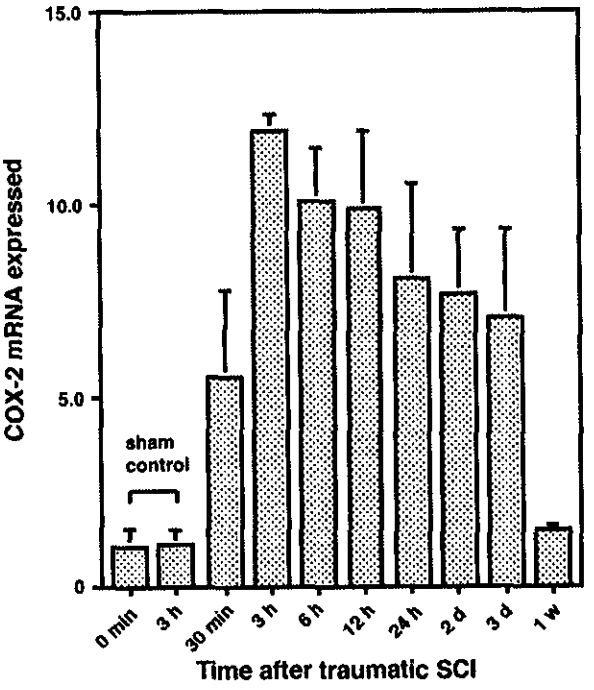

Fig. 1. COX-2 mRNA expression in sham controls and at various times after traumatic spinal cord injury. Data are expressed as the means ± S.E.M. ($n = 3$) of COX-2/β-actin mRNA ratios quantified using Intelligent Quantifier.